CHAPTER 6

CREATION AND TESTING OF AUXILIARY TECHNOLOGICAL EQUIPMENT FOR SOLVING CURRENT PROBLEMS OF LASER WELDING OF THIN-WALLED PRODUCTS MADE OF STAINLESS STEELS

Yurchenko Yu. V.
DOI https://doi.org/10.30525/978-9934-26-653-9-6

INTRODUCTION

The use of sheet metal allows reducing the weight and dimensions of welded structures, as well as decreasing their cost. At the current stage of welding technology development, much attention is paid to welding metals with a wall thickness of less than 2 mm in various structures[1]. Thin sheet metal is traditionally used in industries such as aviation, chemical, food, etc. In aviation, these are pipelines, turbine elements, fuselages, etc.[2],[3]. Every year, hundreds of aircraft are manufactured worldwide, with kilometers of welded joints in their construction. In the chemical industry, these are pipelines, reservoirs, tanks, and vats. These products usually have a significant length of welded joints and increased requirements for their quality. In light industry, particularly in the food industry, most metal products are thin-walled: refrigeration units, pipelines, vessels, tanks, containers for sugar and dairy plants[4],[5]. Thin-

[1] Altenbach H., Eremeyev V. Thin-walled structural elements: Classification, classical and advanced theories, new applications. shell-like structures / ed. by H. Altenbach, V. Eremeyev. Cham: Springer International Publishing, 2017. URL:https://doi.org/10.1007/978-3-319-42277-0_1 (date of access: 17.01.2026)

[2] Shelyagin V.D., Khaskin V.Yu., Bernatsky A.V., Siora, A.V.. Laser welding of thin-wall filter elements of steel 08Kh18N10T. *The Paton Welding Journal,* 2017. Vol. 4. P. 49-52. URL: https://doi.org/10.15407/tpwj2017.04.10 (date of access: 17.01.2026).

[3] Kuczek T. Application of manufacturing constraints to structural optimization of thin-walled structures. Engineering Optimization. 2015. Vol. 48, no. 2. P. 351–360. URL: https://doi.org/10.1080/0305215x.2015.1017350 (date of access: 17.01.2026).

[4] McNair S. a. M., Chaharsooghi A. S., Carnevale M., Rhead A., Onnela A., Daguin J., Cichy K., et al. Manufacturing technologies and joining methods of metallic thin-walled pipes for use in high pressure cooling systems. *The International Journal of Advanced Manufacturing Technology*. 2021. Vol. 118, no. 3–4. P. 667–681. URL: https://doi.org/10.1007/s00170-021-07982-8 (date of access: 17.01.2026).

[5] Wang K., Li L. Structural analysis and optimal design of a spherical thin-walled stainless steel water tank without reinforced tie ribs. *Journal of Vibroengineering*. 2024. Vol. 20, no. 4. P. 983-1000. URL: https://doi.org/10.21595/jve.2024.23812 (date of access: 17.01.2026).

sheet structures are also actively used in automotive engineering, household appliances, construction, medicine, etc. Among the materials most commonly used in these industries, austenitic stainless steels are the most widespread. They account for about two-thirds of global production of stainless steels[6]. Their structure remains austenitic across the entire temperature range – from cryogenic to melting temperatures – due to alloying with nickel, as well as nitrogen and manganese. Austenitic steels are not susceptible to heat hardening, but can be strengthened by cold deformation. They have excellent formability and weldability, are non-magnetic, and retain their ductility at very low temperatures[7],[8]. The most common is the 300 series – chromium-nickel alloys, where the austenitic structure is achieved mainly by adding nickel. The most widespread steels of the austenitic class are AISI 304, AISI 316, and AISI 321. The chemical composition of these steels according to ASTM A480/A480M-22a is given in Table 1.

Table 1

Chemical composition of steels, % by wt.[9]

Grade	C	Si	Mn	Ni	S	P	Cr	Cu	Ti	Mo	Fe
AISI 304	≤0,08	≤0,8	≤2	9 –11	≤0,02	≤0,035	17–19	≤0,3	–	–	Bal.
AISI 316	≤0,03	≤0,4	≤1–2	13–15	≤0,02	≤0,035	16–18	–	–	2,5–3,1	Bal.
AISI 321	≤0,12	≤0,8	≤2	9 –11	≤0,02	≤0,035	17–19	≤0,3	0,4–1	–	Bal.

Stainless steels AISI 304, AISI 316, and AISI 321 are widely used in industry due to their corrosion resistance and high mechanical properties. AISI 304 is the most common grade used in the food industry, household appliances, architecture, and mechanical engineering. AISI 316 contains molybdenum, which increases its resistance to aggressive environments, particularly those containing chlorine, making it the grade of choice for marine, chemical, and medical applications. AISI 321 is alloyed with titanium and is characterized by high heat resistance and resistance to intergranular

[6] Michler T. Austenitic stainless steels. *Reference Module in Materials Science and Materials Engineering.* 2016. Vol. 1, no. 6. URL: https://doi.org/10.1016/b978-0-12-803581-8.02509-1 (date of access: 17.01.2026).

[7] Ibrahim O., Ibrahim I., Khalifa T. Impact behavior of different stainless steel weldments at low temperatures. *Engineering Failure Analysis.* 2010. Vol. 17, no. 5. P. 1069–1076. URL: https://doi.org/10.1016/j.engfailanal.2009.12.006 (date of access: 17.01.2026).

[8] Lv X., Chen S., Wang Q., Jiang H., Rong L. Temperature dependence of fracture behavior and mechanical properties of AISI 316 austenitic stainless steel. *Metals*. 2022. Vol. 12, no. 9. 1421. https://doi.org/10.3390/met12091421 (date of access: 17.01.2026).

[9] ASTM A480/A480M-22a. Standard specification for general requirements for flat-rolled stainless and heat-resisting steel plate, sheet, and strip. Effective from 2023-06-02. Official edition. URL: https://store.astm.org/a0480_a0480m-22a.html (date of access: 17.01.2026).

corrosion, which makes it applicable for use in high-temperature equipment, aviation, and other industries where high operating temperatures are present[10],[11],[12].

Given the properties mentioned above, austenitic steels are most often used for the manufacture of thin-walled structures. To join them, welding processes must be used that ensure minimal heat impact and high-quality welded joints. The main types of welded joints for thin-sheet products are butt joints for flat products and girth joints for cylindrical products.

1. Analysis of the disadvantages of common methods for welding thin-walled products

Today, the most common methods of welding thin-walled products in the world are plasma, electron beam, TIG welding, and MIG welding[13],[14],[15].

Despite the variety of welding processes, the methods described above have their disadvantages. Plasma welding involves high costs for welding equipment and consumables. This can significantly increase the cost of implementing the technology. In addition, achieving the required weld quality requires high precision in joining the welded edges, which complicates the process, especially when it comes to processing thin or long parts[16].

Although electron beam welding is effective, it is not without its disadvantages. The welding equipment for this technology is complex and expensive, making it less accessible for widespread use. In addition, vacuum chambers are required for welding, which limits the ability to process large or

[10] Michler T. Austenitic stainless steels. *Reference Module in Materials Science and Materials Engineering*. 2016. Vol. 1, no. 6. URL: https://doi.org/10.1016/b978-0-12-803581-8.02509-1 (date of access: 17.01.2026).

[11] Ibrahim O., Ibrahim I., Khalifa T. Impact behavior of different stainless steel weldments at low temperatures. *Engineering Failure Analysis*. 2010. Vol. 17, no. 5. P. 1069–1076. URL: https://doi.org/10.1016/j.engfailanal.2009.12.006 (date of access: 17.01.2026).

[12] Lv X., Chen S., Wang Q., Jiang H., Rong L. Temperature dependence of fracture behavior and mechanical properties of AISI 316 austenitic stainless steel. *Metals*. 2022. Vol. 12, no. 9. 1421. https://doi.org/10.3390/met12091421 (date of access: 17.01.2026).

[13] Kumar K., Kumar C. S., Masanta M., Pradhan S. A review on TIG welding technology variants and its effect on weld geometry. *Materials Today Proceedings*. 2021. Vol. 50. P. 999–1004. URL: https://doi.org/10.1016/j.matpr.2021.07.308 (date of access: 17.01.2026).

[14] Advancing implantable medical device reliability with enhanced laser joining technology. *Home – Medical Design Briefs*. URL: https://www.medicaldesignbriefs.com/component/content/article/52177-advancing-implantable-medical-device-reliability-with-enhanced-laser-joining-technology (date of access: 17.01.2026).

[15] Sabdin S. D., Hussein N. I. S., Sued M. K., Ayof M. N. Joining of thin plates using various arc welding heat sources–A Review. *Journal of Advanced Manufacturing Technology (JAMT)*. 2018. Vol. 12, no. 1. P. 357-370. URL: https://jamt.utem.edu.my/jamt/article/view/4005 (date of access: 17.01.2026).

[16] Khoshnaw F. Welding of metallic materials methods, metallurgy, and performance. Elsevier, 2023. 608 p.URL: https://doi.org/10.1016/c2020-0-03713-8 (date of access: 17.01.2026).

heavy products. Since electron beam welding is performed in closed vacuum chambers, complex guidance systems are required for accurate positioning of the electron beam and finding the welding location. The process itself is also accompanied by X-ray radiation, which requires special protective measures for personnel[17].

TIG welding also has its drawbacks. In particular, excessive welding current can cause the tungsten electrode to melt, affecting the quality of the weld by forming brittle tungsten in the weld pool. In addition, this welding process has a low speed, which limits its productivity when welding large-sized products.[18].

Among the main disadvantages of MIG welding is a less stable welding arc, which can lead to an uneven welding process. Another problem is feedback from the welding wire, which can sometimes be uneven, making it difficult to control the welding process. In addition, there may be problems with wire burnout and increased sparking, which can lead to a fire hazard. Welding also produces a large amount of smoke and harmful fumes, requiring the use of appropriate ventilation and personnel protection measures[19].

2. Analysis of the growth and spread of laser tech for welding thin-walled products

Along with the above-mentioned methods of welding thin-walled structures, laser welding is becoming increasingly popular and widely used. Over the past 10 years, laser technologies have developed rapidly, reducing the cost of kilowatt power of laser radiation by approximately 10 times, which has made laser welding even more competitive compared to traditional types of welding[20]. This is confirmed by data from various consulting agencies, which indicate that the global market for laser welding

---

[17] Kumar K., Kumar C. S., Masanta M., Pradhan S. A review on TIG welding technology variants and its effect on weld geometry. *Materials Today Proceedings*. 2021. Vol. 50. P. 999–1004. URL: https://doi.org/10.1016/j.matpr.2021.07.308 (date of access: 17.01.2026).

[18] Manh N. H., Van Anh N., Van Tuan N., Xu B., Akihisa M. Research and development of a novel TIG welding torch for joining thin sheets. *Applied Sciences.* 2019. Vol. 9, no, 23. 5260. URL: https://doi.org/10.3390/app9235260 (date of access: 17.01.2026).

[19] Lv X., Chen S., Wang Q., Jiang H., Rong L. Temperature dependence of fracture behavior and mechanical properties of AISI 316 austenitic stainless steel. *Metals*. 2022. Vol. 12, no. 9. 1421. https://doi.org/10.3390/met12091421 (date of access: 17.01.2026).

[20] Yurchenko, Yu. V., et al. Analysis of actual problems of laser welding of stainless steel thin sheets and search for solutions. *International Journal of Science Engineering and Technology*. 2024. Vol. 12, no. 5. P. 1–9. URL: https://doi.org/10.61463/ijset.vol.12.issue5.289 (date of access: 17.01.2026).

equipment in 2022-2023 amounted to $2.5-2.9 billion[21],[22],[23]. This market is expected to reach approximately $4 billion by 2032, with a compound annual growth rate (CAGR) of 5.5% during the forecast period[24]. The rapid evolution of laser technologies is also confirmed by a significant increase in the number of scientific publications related to laser processing, particularly laser welding.

To assess the spread of lasers in welding technologies, a bibliometric analysis of the Scopus and Google Scholar databases was conducted. The analysis consisted of determining the number of publications covering laser welding processes published between 2014 and 2024. The search was conducted using keywords in two categories: "Laser welding processes" and "Prevalence of laser use." According to the results of the analysis, works devoted to laser welding account for approximately 12% of publications on Google Scholar (90,000) and 17% of publications in the Scopus database (88,850) related to welding materials. At the same time, 51% (340,600 works) of the peer-reviewed publications in Scopus focus on materials processing in industry (Materials Science and Engineering). 24% (160,190 works) are devoted to the use of laser technologies in medicine and biotechnology, and chemical sciences rank third with 16% (108,970 works). This indicates that over the last decade, laser welding processes have become an important and relevant area of scientific research[25].

The main advantages of laser welding are: no need for complex vacuum chambers, highly localized thermal effect, small size of the heat-affected zone, and minimal residual deformation. Fig. 1 shows a comparative diagram of heat-affected zones for different welding methods. It shows that laser welding has one of the smallest heat-affected zones, making this process one of the most optimal for welding thin-walled structures.

---

21 Bala Y., Rajendran D. K. Global welding market growth. *Automation in Welding Industry: Incorporating Artificial Intelligence, Machine Learning and Other Technologies*. 2024. P. 229–243. URL: https://doi.org/10.1002/9781394172948.ch13 (date of access: 17.01.2026).

22 Buang A. S., Bakar M. S. A., Rohani M. Z. A review of trend advanced welding process and welding technology in industries. *International Journal of Technical Vocational and Engineering Technology.* 2024. Vol. 5, no. 1. P. 133-145. URL: https://journal.pktm.com.my/index.php/ijtvet/article/download/103/72 (date of access: 17.01.2026).

23 Rahadian N. Advancements in welding technology: A comprehensive review of techniques, materials, and applications. *Journal PEP Bandung.* 2025.Vol. 2, no. 1. P. 62-110. https://ejournal.pepbandung.ac.id/index.php/gm/article/view/12 (date of access: 17.01.2026).

24 Manh N. H., Van Anh N., Van Tuan N., Xu B., Akihisa M. Research and development of a novel TIG welding torch for joining thin sheets. *Applied Sciences.* 2019. Vol. 9, no, 23. 5260. URL: https://doi.org/10.3390/app9235260 (date of access: 17.01.2026).

25 Yurchenko, Yu. V., et al. Analysis of actual problems of laser welding of stainless steel thin sheets and search for solutions. *International Journal of Science Engineering and Technology*. 2024. Vol. 12, no. 5. P. 1–9. URL: https://doi.org/10.61463/ijset.vol.12.issue5.289 (date of access: 17.01.2026).

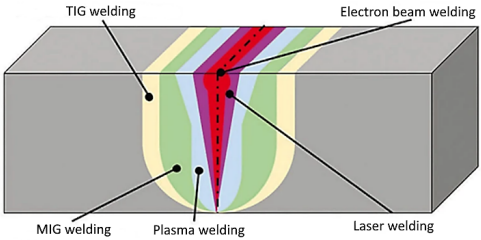

Fig. 1. Heat-affected zone for different welding technologies[26]

Despite the rapid growth of laser welding as a highly productive technology with deep penetration, minimal deformation, and high process speed, a number of technical challenges and problems remain relevant and still don't have a final solution. These include the formation of craters at the beginning and end of the welded joint, ensuring reliable gas protection, effective heat removal, control of welding stresses and deformations, as well as reliable clamping of the welded edges of thin-sheet parts.

3. Analysis of the main problems of laser welding of thin-walled products

3.1. Crater formation in a welded joint

The formation of craters at the end of a welded joint during laser welding remains one of the pressing issues in the manufacture of ring welded joints in thin-walled products. According to EN ISO 6520-1:2007[27], a crater is a cavity that forms at the end of a welded joint under the effect of electric arc pressure and/or gas jet and volumetric shrinkage of metal during its crystallization. In international terminology, this defect is referred to as a «crater» and is shown in Figure 2. The problem of crater formation at the end of a welded joint has been known for a long time, but with the development of welding technologies, thin-walled or closed joints, where it is impossible to use traditional lead-out strips, it is becoming increasingly relevant[28].

---

[26] Advancing implantable medical device reliability with enhanced laser joining technology. *Home – Medical Design Briefs*. URL: https://www.medicaldesignbriefs.com/component/content/article/52177-advancing-implantable-medical-device-reliability-with-enhanced-laser-joining-technology (date of access: 17.01.2026).

[27] EN ISO 6520-1:2007. Welding and allied processes – Classification of geometric imperfections in metallic materials – Part 1: Fusion welding. Effective from 2014-02-15 URL: https://uscc.ua/uploads/page/images/normativnye%20dokumenty/dstu/vigotovlennya-mk-mizhnarodna-gilka-standarty/78-dstu-iso-5817-2016-zvaryuvannya.pdf (date of access: 17.01.2026).

[28] Kenda M., Klobčar D., Nagode A., Bračun D. Analysis and prevention of weld crater cracking in circumferential laser microwelding of automotive pressure sensors. *Engineering Failure Analysis*. 2021. Vol. 128. 105579. URL: https://doi.org/10.1016/j.engfailanal.2021.105579 (date of access: 17.01.2026).

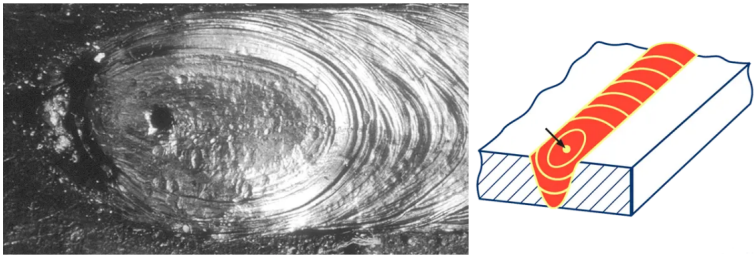

a **b**

Fig. 2. Crater at the end of a welded joint during laser welding: a) top view, b) scheme of the crater of a welded joint[29]

Despite its apparent simplicity, the crater zone is highly complex in terms of thermodynamics, hydrodynamics, metallurgy, and stress-strain state. This is where hot cracks, pores, shrinkage cavities, and microinclusions most often occur, which impair the mechanical properties of the joint, reduce its tightness, and, under unfavorable conditions, can lead to premature failure of the welded joint under load (Fig. 3)[30].

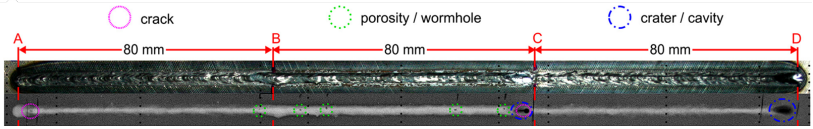

Fig. 3. Defects in welded joints[31]

Controlling the completion of the welding process is particularly challenging. While most technological solutions are aimed at ensuring a stable weld pool in steady state, the completion zone is inherently unstable: after the heat source is turned off, the character of heat flows, temperature distribution, and crystallization rate change, leading to a local loss of balance between phase and hydrodynamic

[29] EN ISO 6520-1:2007. Welding and allied processes – Classification of geometric imperfections in metallic materials – Part 1: Fusion welding. Effective from 2014-02-15 URL: https://uscc.ua/uploads/page/images/normativnye%20dokumenty/dstu/vigotovlennya-mk-mizhnarodna-gilka-standarty/78-dstu-iso-5817-2016-zvaryuvannya.pdf (date of access: 17.01.2026).

[30] Jian G. A. O., Xiaojiao S. O. N. G., Lihua P. A. N., Ling X. I. A., Jie X. U. Study on the quality control of arc crater in laser welding girth weld. *Electric Welding Machine.* 2022. Vol. 52, *no.*5. P. 112-116. URL: http://doi.org/10.7512/j.issn.1001-2303.2022.05.16 (date of access: 17.01.2026).

[31] Lai W. J., Ganguly S., Suder W. Study of the effect of inter-pass temperature on weld overlap start-stop defects and mitigation by application of laser defocusing. *The International Journal of Advanced Manufacturing Technology*. 2021. Vol. 114. P. 117–130. URL: https://doi.org/10.1007/s00170-021-06851-8 (date of access: 17.01.2026).

processes. As a result, the crater becomes a concentrator of residual stresses and a source of crack initiation. In addition to cold cracks, there is also the problem of hot cracks forming during laser welding of austenitic stainless steels[32]. The main reason for their occurrence is the presence in the microstructure of the welded joint of residual molten films with a reduced melting point, which are formed as a result of micro-segregation of low-melting elements such as sulfur, phosphorus, copper, silicon, or the formation of eutectics based on Ni_3S_2, Fe_3P, etc. These films remain in a liquid state even at temperatures significantly lower than the equilibrium solidus temperature of the base material, making them particularly sensitive to mechanical and thermal loads[33]. Under the action of shrinkage stresses arising during cooling or as a result of a rapid change in heat flows in the area of the welded joint, these films lose their integrity, forming hot cracks.

Avoiding crater formation at the beginning and end of a welded joint is an important condition for ensuring high quality and tightness of welded joints, especially during laser welding. One of the key approaches to minimizing craters in laser welding is to adjust the heat balance at the beginning and end of the welded joint.

The most common and effective strategy for avoiding crater formation is to reduce the laser power at the end of the weld (ramp-down). The method of reducing the power of laser radiation at the end of the welded joint allows the temperature in the weld pool to be lowered, promoting uniform crystallization. By reducing temperature gradients and cooling rates, shrinkage stresses are reduced, susceptibility to hot cracks is reduced, and the risk of shrinkage cavities forming in the crater is minimized[34].

In their study, Kenda et al.[35] used three variants of laser radiation power reduction (RD) profiles (Fig. 4). Profile P_1 – classic regime with a linear power reduction of −1.5 W/ms for transition from deep penetration to heat conduction regime. Profile P_2 is a new approach with a zigzag decline: initially to 73% of

[32] Ramon J., Basu R., Voort G. V., Bolar G. A comprehensive study on solidification (hot) cracking in austenitic stainless steel welds from a microstructural approach. *International Journal of Pressure Vessels and Piping*. 2021. Vol. 194. 104560. https://doi.org/10.1016/j.ijpvp.2021.104560 (date of access: 17.01.2026).

[33] Zhang P., Jia Z., Yu Z., Shi H., Li S., Wu D., Tian Y. A review on the effect of laser pulse shaping on the microstructure and hot cracking behavior in the welding of alloys. *Optics & Laser Technology.* 2021. Vol. 140. 107094. URL: https://doi.org/10.1016/j.optlastec.2021.107094 (date of access: 17.01.2026).

[34] Kenda M., Klobčar D., Nagode A., Bračun D. Analysis and prevention of weld crater cracking in circumferential laser microwelding of automotive pressure sensors. *Engineering Failure Analysis*. 2021. Vol. 128. 105579. URL: https://doi.org/10.1016/j.engfailanal.2021.105579 (date of access: 17.01.2026).

[35] Kenda M., Klobčar D., Nagode A., Bračun D. Analysis and prevention of weld crater cracking in circumferential laser microwelding of automotive pressure sensors. *Engineering Failure Analysis*. 2021. Vol. 128. 105579. URL: https://doi.org/10.1016/j.engfailanal.2021.105579 (date of access: 17.01.2026).

power, then 53 Hz modulation with a slope of −0.15 W/ms. Profile P_3 is similar to P_2, but with a frequency of 106 Hz and a slope of −0.25 W/ms.

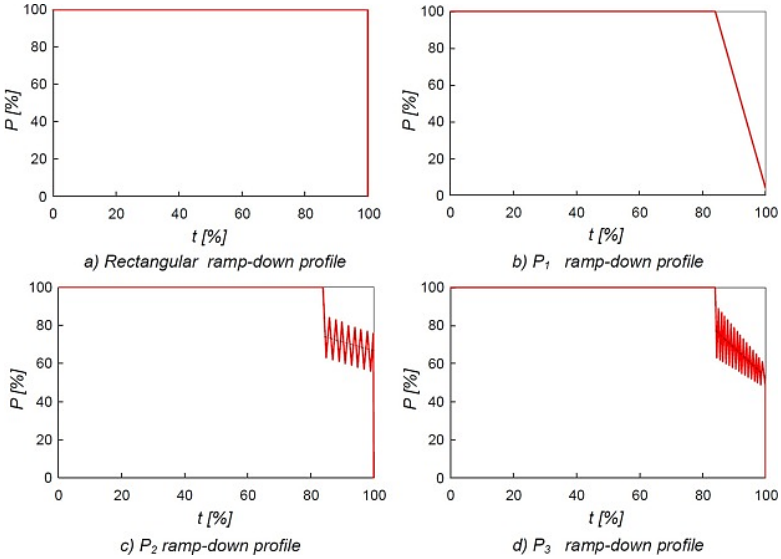

Fig. 4. Laser power reduction profiles: a) rectangular, b) P_1, c) P_2, d) P_3[36]

Fig. 5 shows a top view of three typical welded joint finishes made according to RD profiles P_1, P_2, P_3. When welding with profile P_1, the surface of the welded joint is smooth but has several long axial cracks, which usually occur under such conditions (Fig. 5a). These cracks begin when the power is reduced, and in a certain area of the welded joint, they exist in parallel across the width. The surface of the welded joint when using zigzag profiles P_2 and P_3 (Fig. 5b and 5c) has an arc-shaped structure, i.e., it contains pronounced crystallization zones. The number of such zones corresponds to the number of power modulation cycles embedded in the corresponding RD profile. The images in Fig. 5b and 5c also show that only short surface cracks are formed when zigzag profiles are used. This is because the powerful modulation of the laser beam forms crystallization zones that act as barriers to crack propagation[37].

[36] Kenda M., Klobčar D., Nagode A., Bračun D. Analysis and prevention of weld crater cracking in circumferential laser microwelding of automotive pressure sensors. *Engineering Failure Analysis*. 2021. Vol. 128. 105579. URL: https://doi.org/10.1016/j.engfailanal.2021.105579 (date of access: 17.01.2026).

[37] Kenda M., Klobčar D., Nagode A., Bračun D. Analysis and prevention of weld crater cracking in circumferential laser microwelding of automotive pressure sensors. *Engineering Failure Analysis*. 2021. Vol. 128. 105579. URL: https://doi.org/10.1016/j.engfailanal.2021.105579 (date of access: 17.01.2026).

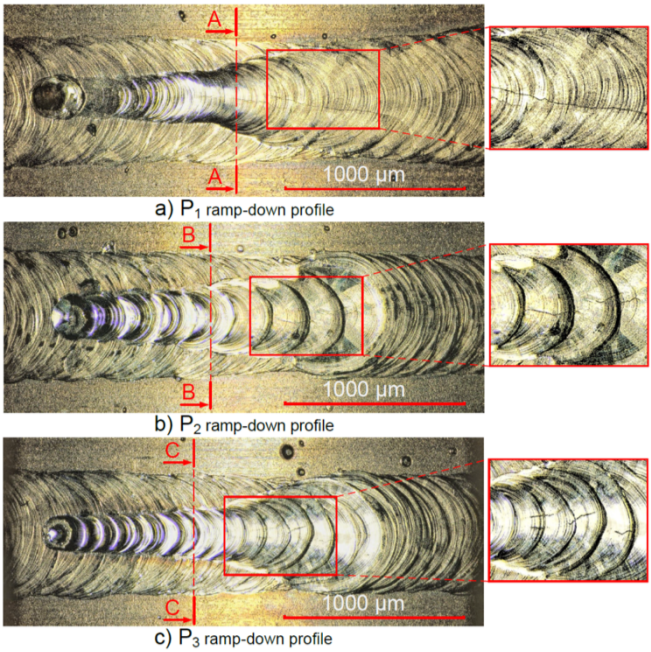

Fig. 5. Comparison of crack morphology on the surface of a welded joint at different laser power reduction profiles: a) P_1; b) P_2; c) P_3 [38]

There are several other methods for avoiding crater formation, including defocusing the laser beam, welding with overlap, and using a "smoothing" weld[39]. The disadvantage of the laser defocusing method is the need to use complicated optical systems in welding heads that ensure controlled change of the focal length. This complicates the design of the equipment, increases its cost and maintenance requirements. The "smoothing" weld method requires an additional pass, which also increases processing time and additional internal stresses due to repeated thermal influence.

Based on the results of a review of scientific works devoted to the study of crater formation at the end of a welded joint, the following conclusion can be drawn. Despite the existence of a certain number of scientific works in this

[38] Kenda M., Klobčar D., Nagode A., Bračun D. Analysis and prevention of weld crater cracking in circumferential laser microwelding of automotive pressure sensors. *Engineering Failure Analysis*. 2021. Vol. 128. 105579. URL: https://doi.org/10.1016/j.engfailanal.2021.105579 (date of access: 17.01.2026).

[39] Gook S., Üstündag Ö., Gumenyuk A., Rethmeier M. Avoidance of end crater imperfections at high-power laser beam welding of closed circumferential welds. Welding in the World. 2019. Vol. 64, no. 2. P. 407–417. URL: https://doi.org/10.1007/s40194-019-00841-x (date of access: 17.01.2026).

area, the topic of crater formation during laser welding of thin-walled welded joints made of stainless steel remains unexplored. Therefore, further research in this area remains relevant.

3.2. Protection of the welding zone to ensure high quality welded joints

The topic of gas protection during welding with concentrated energy sources is relevant because most methods involve welding in the open air without the use of vacuum chambers. Gas protection plays a key role in such cases. Due to the high temperature and localized action of the heat source, even a small amount of air entering the welding zone can lead to the formation of oxide films, pores, cracks, and other defects. This degrades the metal structure and reduces the strength and durability of welded joints[40],[41],[42],[43]. One of the main factors that reduce the effectiveness of gas protection during welding is flow turbulence. When transitioning from laminar to turbulent flow, the protective gas mixes intensively with the surrounding air, causing the oxygen concentration in the welding zone to rise rapidly (Fig. 7)[44],[45]. As a result of pulse exchange at the transition layer with the environment or with the wall (i.e., metal surface), the velocity profile undergoes asymmetric changes with increasing propagation length[46].

Therefore, analysis of surface and free jets allows to evaluate the efficiency of protective gas delivery through flat or tubular nozzles[47].

---

[40] Mahajanam S., Heidersbach K. Corrosion studies of heat-tinted austenitic stainless steel. *Materials Performance*. 2021. Vol. 60, no. 5. P. 42–47. URL:https://doi.org/10.5006/mp2021_60_5-42 (date of access: 17.01.2026).

[41] Kearns J. R. The corrosion of heat tinted austenitic stainless alloys. *Corrosion*. 1985. P. 1–11. URL: https://doi.org/10.5006/c1985-85050 (date of access: 17.01.2026).

[42] Zhang Z., Jing H., Xu L., Han Y., Zhao L., Zhou C. Effects of nitrogen in shielding gas on microstructure evolution and localized corrosion behavior of duplex stainless steel welding joint. *Applied Surface Science*. 2017. Vol. 404. P. 110–128. URL: https://doi.org/10.1016/j.apsusc.2017.01.252 (date of access: 17.01.2026).

[43] Hinds G., Wickström L., Turnbull A. Influence of weld preparation procedure and heat tinting on sulfide stress corrosion cracking of duplex stainless steel. *Corrosion*. 2015. P. 1–15. URL: https://doi.org/10.5006/c2015-06084 (date of access: 17.01.2026).

[44] Schricker K., Baumann A., Bergmann J. P. Local shielding gas supply in remote laser beam welding. *Journal of Manufacturing and Materials Processing*. 2021. Vol. 5, no. 4. 139. URL: https://doi.org/10.3390/jmmp5040139 (date of access: 17.01.2026).

[45] Chen K., Hu Z. H., Huang R., Li M. X., Xiao R. S. Outflow Forms of Shielding Gas in Laser Welding by Schlieren. *Journal of Beijing University of Technology.* 2007. Vol. 33, no. 12. P. 1340-1344. URL: https://journal.bjut.edu.cn/bjgydxxb/en/article/pdf/preview/10.3969/j.issn.0254-0037.2007.12.020.pdf (date of access: 17.01.2026).

[46] Zou J., Xie S., Kong H., Liu T., Fang C., Wu Q. Active control effect of shielding gas flow on high-power fiber laser welding plume. *Journal of Laser Applications*. 2024. Vol. 36, no. 3. 032011. URL: https://doi.org/10.2351/7.0001407 (date of access: 17.01.2026).

[47] Tani G., Ascari A., Campana G., Fortunato A. A study on shielding gas contamination in laser welding of non-ferrous alloys. *Applied Surface Science*. 2007. Vol. 254, no. 4. P. 904–907. URL: https://doi.org/10.1016/j.apsusc.2007.08.067 (date of access: 17.01.2026).

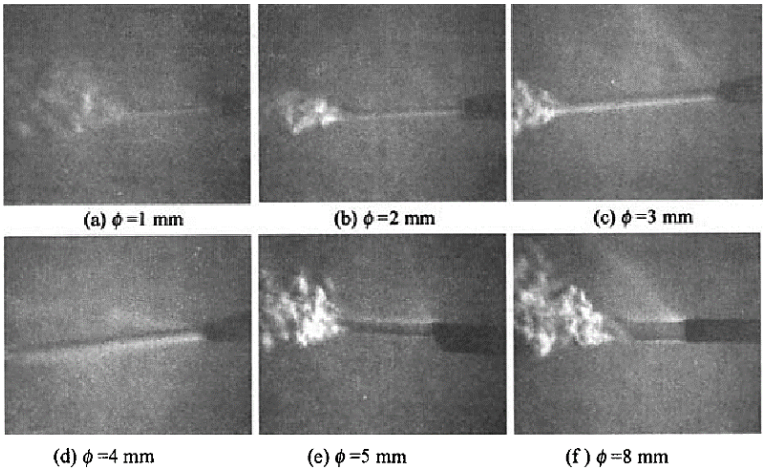

Fig. 6. Characteristics of helium flow depending on nozzle diameter, visualized using schlieren imaging[48]

Near-surface jets demonstrate a significantly longer laminar flow section and less turbulence at the same Reynolds number[49], which indicates the advantage of flat nozzles over other shapes. Depending on the Re value, either stable (Re = 330) or unstable (Re = 370...750) near-surface jets are formed, with higher flow velocities slowing down earlier and being more dependent on external disturbances. The flow rate of the protective gas is one of the most thoroughly studied parameters due to the ease of its regulation. Blackburn et al.[50] found that reducing the flow velocity improves the visual appearance of the weld, as excessive velocity causes turbulence in the gas flow.

Vyskoč[51] investigated the effect of flow velocity on the shape of a weld and found that increasing it reduces the energy absorbed by the plasma

[48] Chen K., Hu Z. H., Huang R., Li M. X., Xiao R. S. Outflow Forms of Shielding Gas in Laser Welding by Schlieren. *Journal of Beijing University of Technology.* 2007. Vol. 33, no. 12. P. 1340-1344. URL: https://journal.bjut.edu.cn/bjgydxxb/en/article/pdf/preview/10.3969/j.issn.0254-0037.2007.12.020.pdf (date of access: 17.01.2026).

[49] Wang S., Zhou Y., Alam M. M., Yang H. Turbulent intensity and Reynolds number effects on an airfoil at low Reynolds numbers. *Physics of Fluids*. 2014. Vol. 26, no. 11. 115107. URL: https://doi.org/10.1063/1.4901969 (date of access: 17.01.2026).

[50] Blackburn J., Allen C., Hilton P., Li L. Nd:YAG laser welding of titanium alloys using a directed gas jet. *Journal of Laser Applications*. 2010. Vol. 22, no. 2. P. 71–78. URL: https://doi.org/10.2351/1.3455825 (date of access: 17.01.2026).

[51] Vyskoč M., Sahul M., Dománková M., Jurči P., Sahul M., Vyskočová M., Martinkovič M. The effect of process parameters on the microstructure and mechanical properties of AW5083 aluminum laser weld joints. *Metals*. 2020. Vol. 10, no. 11. 1443. URL: https://doi.org/10.3390/met10111443 (date of access: 17.01.2026).

torch and at the same time increases the width of the weld. The paper analyzed the relationship between the distance of the shielding gas supply and the porosity of the weld. The optimal supply distance stabilized the vapor-gas channel and reduced porosity. In addition to gas consumption, the researchers also focused on the position of the gas shielding nozzle[52]. Campana et al.[53] concluded that for effective protection, the gas should be supplied at a perpendicular to the workpiece surface, and the nozzle height should be minimized to ensure reliable protection of the vapor-gas channel and the high-temperature welding zone. Grevey et al. investigated the effect of the nozzle angle and found that as the angle decreases, the size of the gas protection zone increases[54].

The most characteristic manifestation of insufficient gas protection of the welding zone is the formation of oxide films on the metal surface, known as heat tint. On stainless steels, such oxide films form at temperatures above 300°C. Their thickness depends on the temperature regime, the duration of heating, and the oxygen content in the weld zone (Fig. 7). Areas with oxide films are characterized by lower corrosion resistance compared to the base metal, which can lead to the formation of local corrosion[55],[56].

The color of oxide films formed during welding varies from light straw to dark blue depending on the temperature. This is due to the formation of oxide films, which are predominantly composed of chromium and iron. During oxidation, alloying elements, in particular chromium, can diffuse to the surface because they oxidize more easily than iron[57].

---

[52] Hamadou M., Fabbro R., Caillibotte G., Chouf K., Briand F. Study of assist gas flow behavior during laser welding. *ICALEO 2002: 21st International Congress on Laser Materials Processing and Laser Microfabrication*. October 14–17, 2002 Scottsdale, Arizona, USA. URL: https://doi.org/10.2351/1.5066140 (date of access: 17.01.2026).

[53] Campana G., Ascari A., Fortunato A., Tani G. Hybrid laser-MIG welding of aluminum alloys: The influence of shielding gases. *Applied Surface Science*. 2008. Vol. 255, no. 10. P. 5588–5590. URL: https://doi.org/10.1016/j.apsusc.2008.07.169 (date of access: 17.01.2026).

[54] Grevey D., Sallamand P., Cicala E., Ignat S. Gas protection optimization during Nd:YAG laser welding. *Optics & Laser Technology*. 2004. Vol. 37, no.8. P. 647–651. URL: https://doi.org/10.1016/j.optlastec.2004.08.015 (date of access: 17.01.2026).

[55] Kearns J. R. The corrosion of heat tinted austenitic stainless alloys. *Corrosion*. 1985. P. 1–11. URL: https://doi.org/10.5006/c1985-85050 (date of access: 17.01.2026).

[56] Elshawesh F., Elhoud A. Role of heat tint on pitting corrosion of 304 austenitic stainless steel in chloride environment (No. INIS-FR--3844). Societe de Chimie Industrielle (SCI), 28 Rue Saint Dominique, F-75007 Paris (France). 2004. URL: https://inis.iaea.org/records/016t7-4rr25 (date of access: 17.01.2026).

[57] Mahajanam S., Heidersbach K. Corrosion studies of heat-tinted austenitic stainless steel. *Materials Performance*. 2021. Vol. 60, no. 5. P. 42–47. URL:https://doi.org/10.5006/mp2021_60_5-42 (date of access: 17.01.2026).

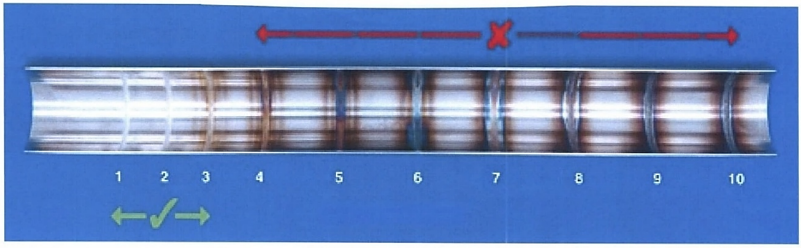

Fig. 7. Colors of oxide films on the surface of stainless steel[58]

As a result, an area with reduced chromium content forms under the film, which negatively affects the corrosion resistance of this area compared to the rest of the steel volume[59]. The rate of oxidation and the level of depletion of alloying elements in the area under the film are determined not by the overall chemical composition of the steel, but by the properties of the oxide film itself, in particular its ability to diffuse[60]. Heterogeneous oxides consisting mainly of chromium and iron form on the surface. They are located above the metal that has already lost some of the chromium. Due to its heterogeneous structure, the presence of defects and internal stresses, such an oxide film does not provide reliable protection against corrosion. In certain environments, this can lead to local corrosion in the area with reduced chromium content located under the film[61]. During service, welded joints made of stainless steel may be exposed to various types of corrosion, namely pitting, crevice, intergranular, and stress corrosion[62],[63],[64]. A protective passive film on the

[58] Tran N., Nguyen V., Nguyen V., Trung T., DO, Nguyen V., Nguyen V. Effects of heat input and backing gas on bead geometry and weld heat tint in sanitary tube welding. *Thermo.* 2025. Vol. 5, no. 4. 49. URL: https://doi.org/10.3390/thermo5040049 (date of access: 17.01.2026).

[59] Ciofu F., Nioata A., Luca L. Duplex stainless steel corrosion resistance. *Fascicle of Management of Technological Engineering*. 2010. Vol. 9. URL: https://imt.uoradea.ro/auo.fmte/files-2010-v2/TCM/Ciofu%20Florin%20L2.pdf (date of access: 17.01.2026).

[60] Olsson C., Landolt D. Passive films on stainless steels–chemistry, structure and growth. *Electrochimica Acta*. 2003. Vol. 48, no. 9. P. 1093–1104. URL: https://doi.org/10.1016/s0013-4686(02)00841-1 (date of access: 17.01.2026).

[61] Morcillo M., Díaz I., Cano H., Chico B., De La Fuente D. Atmospheric corrosion of weathering steels. Overview for engineers. Part I: Basic concepts. *Construction and Building Materials*. 2019. Vol. 213. P. 723–737. URL: https://doi.org/10.1016/j.conbuildmat.2019.03.334 (date of access: 17.01.2026).

[62] Kearns J. R. The corrosion of heat tinted austenitic stainless alloys. *Corrosion*. 1985. P. 1–11. URL: https://doi.org/10.5006/c1985-85050 (date of access: 17.01.2026).

[63] Aljohani T. A., Alateyah A., El-Sanabary S., El-Garaihy W. Corrosion of weldments. *Welding of Metallic Materials: Methods, Metallurgy, and Performance*. 2023. P. 565–588. URL: https://doi.org/10.1016/b978-0-323-90552-7.00010-9 (date of access: 17.01.2026).

[64] Zhu L., Cui Z., Cui H., Wang X., Li Y. The effect of applied stress on the crevice corrosion of 304 stainless steel in 3.5 wt% NaCl solution. *Corrosion Science*. 2022. Vol. *196*. 110039. URL: https://doi.org/10.1016/j.corsci.2021.110039 (date of access: 17.01.2026).

surface of stainless steel provides high resistance to uniform corrosion in typical oxidizing environments[65],[66],[67]. However, in the presence of aggressive factors, local destruction of this film is possible, leading to the formation of pitting corrosion[68],[69]. The effect of high temperatures in the range of 500–800 °C (so-called «critical temperatures») during welding followed by slow cooling in air makes 2 mm thick austenitic corrosion-resistant steel AISI 304 susceptible to intergranular corrosion[70],[71],[72].

Under these conditions, chromium carbides precipitate along the grain boundaries, reducing the chromium content in the adjacent area (Fig. 8). If the chromium concentration decreases below the critical level for passivation (approximately 11.5%), this area becomes anodic relative to the rest of the grain, leading to sensitization of the material and its susceptibility to intergranular corrosion[73]. Areas with chromium depletion may also become pathways for the preferential formation of other types of localized corrosion or crack propagation in the presence of tensile stresses[74].

---

65 Wang X., Sun Y., He P., Tan X., Zhou Q., Wu W., Lv C., Li J., Jiang Y. Understanding the pitting behavior of laser welds in different austenitic stainless steels: From the perspective of pitting initiation. *Corrosion Science*. 2023. Vol. 224, 111483. URL: https://doi.org/10.1016/j.corsci.2023.111483 (date of access: 17.01.2026).

66 Sun L., Chen S., Qiu J., Zhao T. Research on the mechanism and detection method of intergranular corrosion of AISI 304 stainless steel by electrochemical techniques in heat exchanger equipment. *Journal of Materials Engineering and Performance*. 2022. Vol. 32, no. 2. P. 534–543. URL: https://doi.org/10.1007/s11665-022-07132-5 (date of access: 17.01.2026).

67 Kappes M. A. Localized corrosion and stress corrosion cracking of stainless steels in halides other than chlorides solutions: a review. *Corrosion Reviews*. 2019. Vol. 38, no. 1. P. 1–24. URL: https://doi.org/10.1515/corrrev-2019-0061 (date of access: 17.01.2026).

68 Wang X., Sun Y., He P., Tan X., Zhou Q., Wu W., Lv C., Li J., Jiang Y. Understanding the pitting behavior of laser welds in different austenitic stainless steels: From the perspective of pitting initiation. *Corrosion Science*. 2023. Vol. 224, 111483. URL: https://doi.org/10.1016/j.corsci.2023.111483 (date of access: 17.01.2026).

69 Aghuy A. A., Zakeri M., Moayed M., Mazinani M. Effect of grain size on pitting corrosion of 304L austenitic stainless steel. *Corrosion Science*. 2015. Vol. 94. P. 368–376. URL: https://doi.org/10.1016/j.corsci.2015.02.024 (date of access: 17.01.2026).

70 Sun L., Chen S., Qiu J., Zhao T. Research on the mechanism and detection method of intergranular corrosion of AISI 304 stainless steel by electrochemical techniques in heat exchanger equipment. *Journal of Materials Engineering and Performance*. 2022. Vol. 32, no. 2. P. 534–543. URL: https://doi.org/10.1007/s11665-022-07132-5 (date of access: 17.01.2026).

71 Srinivasan N. Sensitization of Austenitic Stainless steels: current developments, trends, and future directions. *Metallography Microstructure and Analysis*. (2021). Vol. 10, no. 2. P. 133–147. URL: https://doi.org/10.1007/s13632-021-00724-y (date of access: 17.01.2026).

72 Shit G., Mariappan K., Ningshen S. Improvement of sensitization and intergranular corrosion of AISI type 304L stainless steel through thermo-mechanical treatment. *Corrosion Science*. 2023. Vol. 213. 110975. URL: https://doi.org/10.1016/j.corsci.2023.110975 (date of access: 17.01.2026).

73 Shit G., Mariappan K., Ningshen S. Improvement of sensitization and intergranular corrosion of AISI type 304L stainless steel through thermo-mechanical treatment. *Corrosion Science*. 2023. Vol. 213. 110975. URL: https://doi.org/10.1016/j.corsci.2023.110975 (date of access: 17.01.2026).

74 Vakili M., Koutník P., Kohout J., Gholami Z. Analysis, assessment, and mitigation of stress corrosion cracking in austenitic stainless steels in the oil and gas sector: a review. *Surfaces*. 2024. Vol. 7, no. 3. P. 589–642. URL: https://doi.org/10.3390/surfaces7030040 (date of access: 17.01.2026).

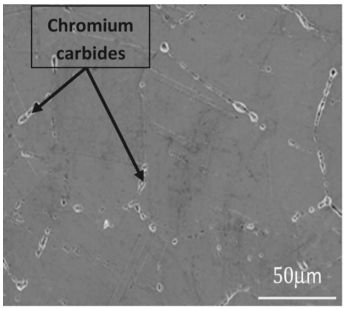

Fig. 8. SEM image of chromium carbides at the grain boundaries of AISI 304 steel[75]

Special gas protection systems are used to prevent the formation of oxide films on the metal surface during welding and to reduce the likelihood of corrosion damage. They ensure the supply of protective gas to the welding area in order to isolate the molten metal and adjacent areas from contact with oxygen, nitrogen, and moisture from the environment. The development of effective gas protection devices is a relevant area of research, since the quality of a welded joint significantly depends on the stability and uniformity of the gas flow. A number of scientific papers have proposed technical solutions aimed at forming a laminar flow of shielding gas, which increases the effectiveness of protection and minimizes the formation of defects in the welded joint[76],[77],[78].

One of the main ways to make reliable gas protection is to gradually create a steady laminar flow. To start with, diffusers made of sintered metal or metal foam are used to even out the gas speed. These diffusers really cut down on flow turbulence and make the gas spread out more evenly (Fig. 9)[79]. Depending on

[75] Sun L., Chen S., Qiu J., Zhao T. Research on the mechanism and detection method of intergranular corrosion of AISI 304 stainless steel by electrochemical techniques in heat exchanger equipment. *Journal of Materials Engineering and Performance*. 2022. Vol. 32, no. 2. P. 534–543. URL: https://doi.org/10.1007/s11665-022-07132-5 (date of access: 17.01.2026).

[76] Schricker K., Baumann A., Bergmann J. P. Local shielding gas supply in remote laser beam welding. *Journal of Manufacturing and Materials Processing*. 2021. Vol. 5, no. 4. 139. URL: https://doi.org/10.3390/jmmp5040139 (date of access: 17.01.2026).

[77] Derakhshan E. D., Yazdian N., Craft B., Smith S., Kovacevic R. Numerical simulation and experimental validation of residual stress and welding distortion induced by laser-based welding processes of thin structural steel plates in butt joint configuration. *Optics & Laser Technology*. 2018. Vol. 104. P. 170–182. URL: https://doi.org/10.1016/j.optlastec.2018.02.026 (date of access: 17.01.2026).

[78] Vykhtar B., Lingner M., Richter A. M., Hoops F. Monitoring and local gas shielding at laser-based welding of titanium alloys. *Procedia CIRP*. 2022. Vol. 111. P. 532–535. URL: https://doi.org/10.1016/j.procir.2022.08.085 (date of access: 17.01.2026).

[79] Schricker K., Baumann A., Bergmann J. P. Local shielding gas supply in remote laser beam welding. *Journal of Manufacturing and Materials Processing*. 2021. Vol. 5, no. 4. 139. URL: https://doi.org/10.3390/jmmp5040139 (date of access: 17.01.2026).

the requirements for protection quality and nozzle design, it is possible to use both individual elements and their combinations. For example, a honeycomb structure can be installed after the diffuser to direct the flow along the nozzle axis, effectively reducing transverse velocity fluctuations. At the same time, to achieve sufficient stabilization, a ratio of cell length to diameter of at least 5:1 is selected, which suppresses turbulence and promotes the formation of laminar flow[80]. It is important to avoid abrupt changes in the shape and cross-section of the internal channels of the nozzle. The transition areas between sections are made with radius, which reduces the probability of flow disruption and the formation of new areas of turbulence. Such a smooth direction ensures a uniform laminar flow, especially if the channel length is sufficient to form a full parabolic velocity profile (Fig. 9)[81].

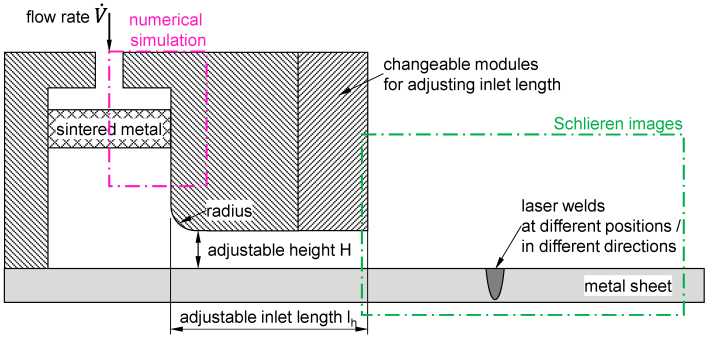

Fig. 9. Schematic cross-section of a protective nozzle with radiused edges and a sintered metal diffuser[82]

Another common technique is to use multiple directions for supplying protective gas. Gas is supplied both directly to the welding area and to the surrounding space. This is achieved through separate channels: one directed straight at the welding area, another at an angle or opposite to the direction of the beam to prevent air ingress, and a third through the central chamber with subsequent distribution

[80] Derakhshan E. D., Yazdian N., Craft B., Smith S., Kovacevic R. Numerical simulation and experimental validation of residual stress and welding distortion induced by laser-based welding processes of thin structural steel plates in butt joint configuration. *Optics & Laser Technology*. 2018. Vol. 104. P. 170–182. URL: https://doi.org/10.1016/j.optlastec.2018.02.026 (date of access: 17.01.2026).

[81] Schricker K., Baumann A., Bergmann J. P. Local shielding gas supply in remote laser beam welding. *Journal of Manufacturing and Materials Processing*. 2021. Vol. 5, no. 4. 139. URL: https://doi.org/10.3390/jmmp5040139 (date of access: 17.01.2026).

[82] Schricker K., Baumann A., Bergmann J. P. Local shielding gas supply in remote laser beam welding. *Journal of Manufacturing and Materials Processing*. 2021. Vol. 5, no. 4. 139. URL: https://doi.org/10.3390/jmmp5040139 (date of access: 17.01.2026).

through a honeycomb structure. In addition, the devices are equipped with welding fume extraction systems that do not interfere with the main flow of shielding gas. For this purpose, extraction nozzles are used, which remove gas only from the periphery, leaving the central zone with a clean inert environment[83].

A review of scientific works on gas protection shows that there are currently studies devoted to the general patterns of laminar flow formation during welding with a relatively large gap between the clamping plates. However, the development of devices capable of ensuring an effective laminar gas flow in a narrow gap between closely spaced clamping plates of the clamping device remains outside the scope of research. This confirms the relevance of creating gas protection devices for such welding conditions.

3.3. Formation of welding stresses and deformations

Welding with highly concentrated energy sources inevitably leads to residual stresses and deformations after cooling of the weld zone. Localized heat influence and subsequent uneven cooling cause internal stresses and deformations that can significantly affect the geometric accuracy and strength of structures[84]. Figure 10 shows typical forms of deformation that occur during the welding of flat parts.

Transverse and longitudinal shrinkage, as well as angular distortion, are the three main types of welding deformation that are commonly combined in real welded structures[85].

In particular, Figure 11a shows the distribution of longitudinal residual stresses (in the direction of welding) both along the weld and at the cross section in its center. The maximum tensile residual stress is recorded in the area around the weld line. Compressive stresses are formed in areas distant from the weld zone to maintain equilibrium. Along the weld line, the residual stresses at its ends decrease to zero due to free boundaries. Similarly, Figure 11b shows the distribution of transverse residual stress: it is tensile in the center and compressive at the beginning and end of the weld, and approaches zero at the edges of the plate[86].

---

[83] Vykhtar B., Lingner M., Richter A. M., Hoops F. Monitoring and local gas shielding at laser-based welding of titanium alloys. *Procedia CIRP*. 2022. Vol. 111. P. 532–535. URL: https://doi.org/10.1016/j.procir.2022.08.085 (date of access: 17.01.2026).

[84] Huang H., Tsutsumi S., Wang J., Li L., Murakawa H. High performance computation of residual stress and distortion in laser welded 301L stainless sheets. *Finite Elements in Analysis and Design*. 2017. Vol. 135. P. 1–10. URL: https://doi.org/10.1016/j.finel.2017.07.004 (date of access: 17.01.2026).

[85] Murakawa H. Residual stress and distortion in laser welding. *Handbook of Laser Welding Technologies*. 2013. P. 374–400. URL: https://doi.org/10.1533/9780857098771.2.374 (date of access: 17.01.2026).

[86] Murakawa H. Residual stress and distortion in laser welding. *Handbook of Laser Welding Technologies*. 2013. P. 374–400. URL: https://doi.org/10.1533/9780857098771.2.374 (date of access: 17.01.2026).

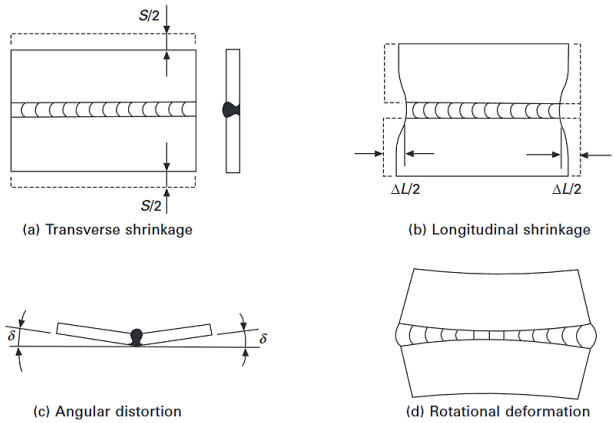

Fig. 10. Typical deformations during welding: (a) transverse shrinkage; (b) longitudinal shrinkage; (c) angular deformation; (d) rotational deformation[87]

The level of welding deformations and residual stresses is largely determined by the amount of heat input. As a rule, with an increase in heat input, both residual stresses and the degree of deformation increase[88]. In this sense, laser welding, which is characterized by high energy density, is advantageous because it requires less heat input compared to other welding methods.[89].

The evolution of residual stresses during welding is related to the interaction of metallurgical changes and microstructure morphology. Tensile residual stresses have a negative effect on structural integrity, while compressive residual stresses usually have a positive effect, in particular increasing fatigue strength[90],[91]. The change in stress caused by grain size may be a consequence

[87] Murakawa H. Residual stress and distortion in laser welding. *Handbook of Laser Welding Technologies*. 2013. P. 374–400. URL: https://doi.org/10.1533/9780857098771.2.374 (date of access: 17.01.2026).

[88] Liu Z., Jin X., Li J., Hao Z., Zhang J. Numerical simulation and experimental analysis on the deformation and residual stress in trailing ultrasonic vibration assisted laser welding. *Advances in Engineering Software*. 2022. Vol. 172. 103200. URL: https://doi.org/10.1016/j.advengsoft.2022.103200 (date of access: 17.01.2026).

[89] Tayebi M., Soltani H. M., Rajaee A. Laser welding. In *IntechOpen eBooks*. 2022. URL: https://doi.org/10.5772/intechopen.102456 (date of access: 17.01.2026).

[90] Kumar B., Bag S., Mahadevan S., Paul C., Das C., Bindra K. On the interaction of microstructural morphology with residual stress in fiber laser welding of austenitic stainless steel. *CIRP Journal of Manufacturing Science and Technology*. 2021. Vol. 33. P. 158–175. URL: https://doi.org/10.1016/j.cirpj.2021.03.009 (date of access: 17.01.2026).

[91] Chiocca A., Frendo F., Bertini L. Residual stresses influence on the fatigue strength of structural components. *Procedia Structural Integrity*. 2022. Vol. 38. P. 447–456. URL: https://doi.org/10.1016/j.prostr.2022.03.045 (date of access: 17.01.2026).

of variations in the properties of the austenitic and ferritic phases, in particular elastic deformation, thermal and plastic mismatch. At the same time, the crystal lattice parameter, which is a function of the interstitial atom content, is crucial for interpreting the desired residual stress in expanded austenite of AISI 316 steel[92]. On the other hand, it has been proven that solid-phase transformation has a certain effect on the distribution of residual stresses in AISI 304 steel, but this effect is not significant[93].

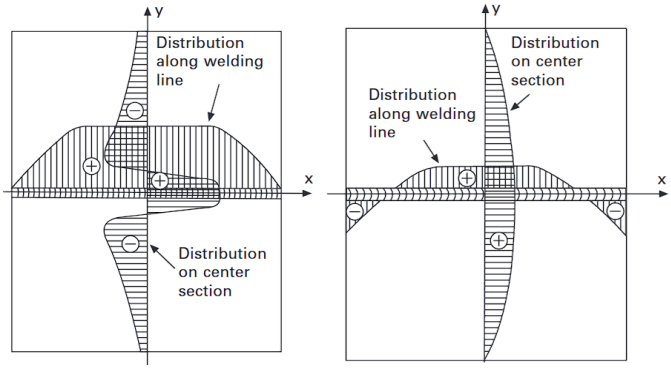

a **b**

Fig. 11. Scheme of residual stress distribution during welding: (a) stress in the welding direction, (b) stress in the transverse direction[94]

The study[95] examined the effect of microstructure and heat input on residual stresses after laser welding of 1 mm thick AISI 304 stainless steel. During the research, laser welding was performed with a constant laser power of 750 W, while the welding speed was varied in the range of 0.6...1 m/min, and the defocusing value was varied in the range of 0...-1 mm. It was found that a ratio of chromium to nickel equivalents of about 1.69 confirms a ferrite-austenite

[92] Hummelshøj T. S., Christiansen T. L., Somers M. A. Lattice expansion of carbon-stabilized expanded austenite. *Scripta Materialia*. 2010. Vol. 63, no. 7. P. 761–763. URL: https://doi.org/10.1016/j.scriptamat.2010.05.031 (date of access: 17.01.2026).

[93] Lin Y., Chou C. A new technique for reducing the residual stress induced by welding in type 304 stainless steel. *Journal of Materials Processing Technology*. 1995. Vol. 48, no. 1–4. P. 693–698. URL: https://doi.org/10.1016/0924-0136(94)01710-i (date of access: 17.01.2026).

[94] Murakawa H. Residual stress and distortion in laser welding. *Handbook of Laser Welding Technologies*. 2013. P. 374–400. URL: https://doi.org/10.1533/9780857098771.2.374 (date of access: 17.01.2026).

[95] Kumar B., Bag S., Mahadevan S., Paul C., Das C., Bindra K. On the interaction of microstructural morphology with residual stress in fiber laser welding of austenitic stainless steel. *CIRP Journal of Manufacturing Science and Technology*. 2021. Vol. 33. P. 158–175. URL: https://doi.org/10.1016/j.cirpj.2021.03.009 (date of access: 17.01.2026).

type crystallization mode, in which the microstructure consists of a combined phase of needle-like and lath δ-ferrite in an austenitic matrix. The maximum δ-ferrite content (12%) is achieved at the lowest heat input of 45 J/mm, while at an increase to 75 J/mm, its amount decreases to 7–8%. With increasing heat input, the thickness of dendrites increases from 484 nm to 927 nm, and the interdendritic interval doubles from 3 to 6 μm, while lath δ-ferrite decreases in favor of needle-like δ-ferrite (Fig. 12). The highest quality welded joint is observed with minimal heat input, which is explained by a very fine dendritic structure and minimal inter-dendritic spacing. The higher coefficient of thermal expansion of nickel compared to chromium causes tensile stresses in the γ-austenite phase and compressive stresses in the δ-ferrite dendritic phase.

At low heat input, which increases the chromium content and reduces nickel, compressive stresses arise, which contribute to a reduction in residual stresses. Also, reducing the heat input from 75 to 45 J/mm reduces the longitudinal tensile stresses to 245 MPa, which is below the yield strength, and the transverse residual stresses change from tensile to compressive (Fig. 13)[96].

Several approaches can be used to reduce stress and deformation levels. For example, the use of closely spaced external clamping plates when welding straight welded pipe joints. External clamping plates significantly reduce residual stresses and welding deformations by more than 30% compared to not using clamping plates.[97]. The use of copper backing plates on the back side of welded joints also significantly reduces residual stresses and deformations[98].

Based on the results of a literature review of contemporary scientific works on laser welding of thin-walled parts, the following areas for further research were identified:

1. Gas protection during laser welding of thin-walled products in a narrow gap between clamping plates is important to prevent the formation of oxide films, pores, and a decrease in the corrosion resistance of joints. Currently, there are studies devoted to the general patterns of laminar flow formation during welding with a relatively wide gap between the clamping

[96] Kumar B., Bag S., Mahadevan S., Paul C., Das C., Bindra K. On the interaction of microstructural morphology with residual stress in fiber laser welding of austenitic stainless steel. *CIRP Journal of Manufacturing Science and Technology*. 2021. Vol. 33. P. 158–175. URL: https://doi.org/10.1016/j.cirpj.2021.03.009 (date of access: 17.01.2026).

[97] Mandal N.R. Welding Residual Stress and Distortion. *Ship Construction and Welding. Springer Series on Naval Architecture, Marine Engineering, Shipbuilding and Shipping.* 2017. Vol. 2. Springer URL: https://doi.org/10.1007/978-981-10-2955-4_17 (date of access: 17.01.2026).

[98] Mohammed M. S., Hamdey M. D., Kareem A. H., Majdi H. S. Investigation of copper backing plate effects in stainless steel welding distortion, heat distribution, and residual stress. *International Journal of Heat and Technology*. 2024. Vol. 42, no. 4. P. 1434–1446. URL: https://doi.org/10.18280/ijht.420433 (date of access: 17.01.2026).

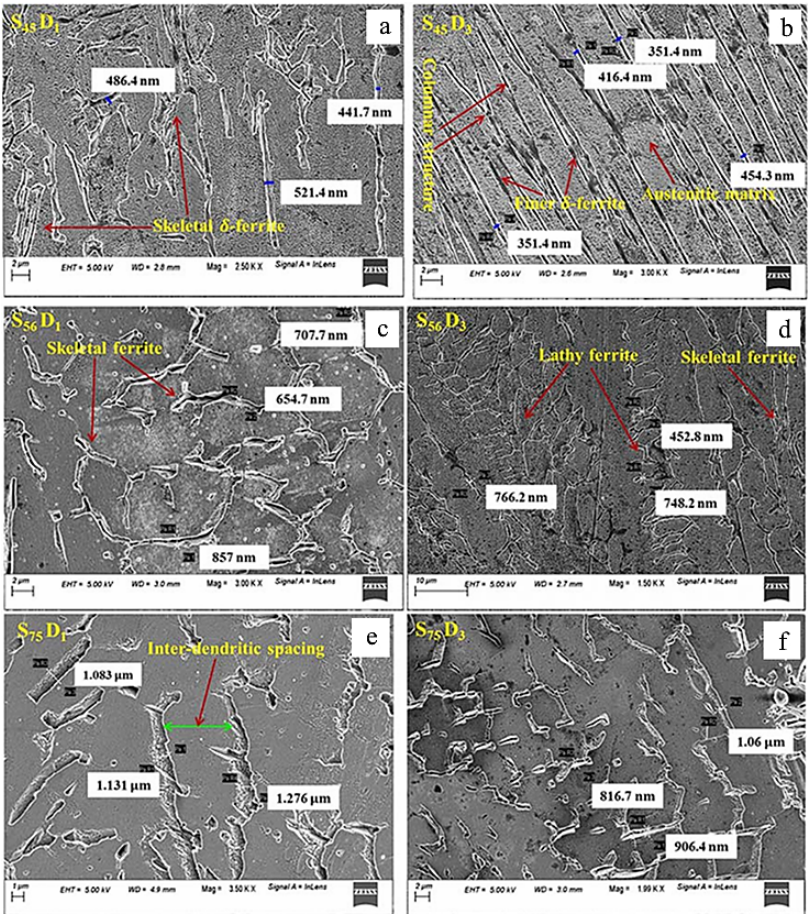

Fig. 12. Variation of the primary dendritic lattice of δ-ferrite under different welding parameters for 1 mm thick AISI 304 steel: a) P = 750 W, V = 1 m/min, ΔF = 0 mm; b) P = 750 W, V = 1 m/min, ΔF = -1 mm; c) P = 750 W, V = 0.8 m/min, ΔF = 0 mm; d) P = 750 W, V = 0.8 m/min, ΔF = -1 mm; e) P = 750 W, V = 0.6 m/min, ΔF = 0 mm; f) P = 750 W, V = 0.6 m/min, ΔF = -1 mm [99]

[99] Kumar B., Bag S., Mahadevan S., Paul C., Das C., Bindra K. On the interaction of microstructural morphology with residual stress in fiber laser welding of austenitic stainless steel. *CIRP Journal of Manufacturing Science and Technology*. 2021. Vol. 33. P. 158–175. URL: https://doi.org/10.1016/j.cirpj.2021.03.009 (date of access: 17.01.2026).

plates[100],[101],[102]. However, the development of devices capable of ensuring an effective laminar gas flow in the narrow gap between closely spaced clamping plates remains outside the scope of research. This confirms the relevance of creating gas protection devices for such welding conditions. To reduce turbulence in the flow and ensure stable and constant gas protection in the welding zone, it is promising to use additional gas distribution elements in the design of gas protection devices based on metal meshes or sintered porous metal, which allow stabilizing the speed and reducing the intensity of mixing with atmospheric air[103],[104]. The ratio of the diameter to the length of the outlet channel also plays an important role, which must be at least 1:5 to ensure laminar flow stability[105]. Further research should focus on developing a gas protection device for welding in conditions of a narrow gap between the clamping plates, which would ensure a stable laminar flow of protective gas.

2. The problem of deformation and residual stresses in thin-walled welded structures is particularly critical due to the low rigidity of the elements and high sensitivity to thermal effects. Even when using laser welding with a lower level of heat input compared to other welding methods, deformations caused by a concentrated heat source can lead to a loss of geometric accuracy and strength of products and welded joints, respectively[106],[107]. Among the known solutions, the most effective are the use of copper backing plates, which, due to their high thermal conductivity, ensure effective heat dissipation and reduce the size of

---

100 Schricker K., Baumann A., Bergmann J. P. Local shielding gas supply in remote laser beam welding. *Journal of Manufacturing and Materials Processing*. 2021. Vol. 5, no. 4. 139. URL: https://doi.org/10.3390/jmmp5040139 (date of access: 17.01.2026).

101 Derakhshan E. D., Yazdian N., Craft B., Smith S., Kovacevic R. Numerical simulation and experimental validation of residual stress and welding distortion induced by laser-based welding processes of thin structural steel plates in butt joint configuration. *Optics & Laser Technology*. 2018. Vol. 104. P. 170–182. URL: https://doi.org/10.1016/j.optlastec.2018.02.026 (date of access: 17.01.2026).

102 Vykhtar B., Lingner M., Richter A. M., Hoops F. Monitoring and local gas shielding at laser-based welding of titanium alloys. *Procedia CIRP*. 2022. Vol. 111. P. 532–535. URL: https://doi.org/10.1016/j.procir.2022.08.085 (date of access: 17.01.2026).

103 Schricker K., Baumann A., Bergmann J. P. Local shielding gas supply in remote laser beam welding. *Journal of Manufacturing and Materials Processing*. 2021. Vol. 5, no. 4. 139. URL: https://doi.org/10.3390/jmmp5040139 (date of access: 17.01.2026).

104 Derakhshan E. D., Yazdian N., Craft B., Smith S., Kovacevic R. Numerical simulation and experimental validation of residual stress and welding distortion induced by laser-based welding processes of thin structural steel plates in butt joint configuration. *Optics & Laser Technology*. 2018. Vol. 104. P. 170–182. URL: https://doi.org/10.1016/j.optlastec.2018.02.026 (date of access: 17.01.2026).

105 Vykhtar B., Lingner M., Richter A. M., Hoops F. Monitoring and local gas shielding at laser-based welding of titanium alloys. *Procedia CIRP*. 2022. Vol. 111. P. 532–535. URL: https://doi.org/10.1016/j.procir.2022.08.085 (date of access: 17.01.2026).

106 Huang H., Tsutsumi S., Wang J., Li L., Murakawa H. High performance computation of residual stress and distortion in laser welded 301L stainless sheets. *Finite Elements in Analysis and Design*. 2017. Vol. 135. P. 1–10. URL: https://doi.org/10.1016/j.finel.2017.07.004 (date of access: 17.01.2026).

107 Murakawa H. Residual stress and distortion in laser welding. *Handbook of Laser Welding Technologies*. 2013. P. 374–400. URL: https://doi.org/10.1533/9780857098771.2.374 (date of access: 17.01.2026).

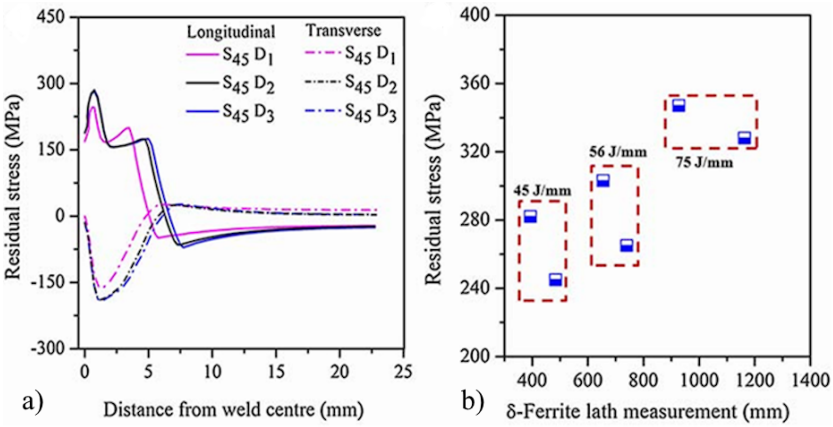

Fig. 13. a) distribution of residual stresses at the lowest heat input of 45 J/mm, b) change in the size of primary δ-ferrite dendrites depending on residual stress[108]

the heat-affected zone, as well as the optimization of laser welding parameters, which reduce the levels of stress and deformation in welded products[109],[110],[111]. An important condition for the effectiveness of these solutions is the optimal placement of the clamping plates and ensure that the parts fit completely to the copper backing plate. Further research may be directed toward studying the stresses and strains in the welded part at different distances between the clamping plates.

3. The formation of craters at the end of a welded joint during laser welding remains one of the major problems in the manufacture of girth welded joints in thin-walled products. Despite the existence of research, the main focus in

[108] Kumar B., Bag S., Mahadevan S., Paul C., Das C., Bindra K. On the interaction of microstructural morphology with residual stress in fiber laser welding of austenitic stainless steel. *CIRP Journal of Manufacturing Science and Technology*. 2021. Vol. 33. P. 158–175. URL: https://doi.org/10.1016/j.cirpj.2021.03.009 (date of access: 17.01.2026).

[109] Kumar B., Bag S., Mahadevan S., Paul C., Das C., Bindra K. On the interaction of microstructural morphology with residual stress in fiber laser welding of austenitic stainless steel. *CIRP Journal of Manufacturing Science and Technology*. 2021. Vol. 33. P. 158–175. URL: https://doi.org/10.1016/j.cirpj.2021.03.009 (date of access: 17.01.2026).

[110] Mandal N.R. Welding Residual Stress and Distortion. *Ship Construction and Welding. Springer Series on Naval Architecture, Marine Engineering, Shipbuilding and Shipping.* 2017. Vol. 2. Springer URL: https://doi.org/10.1007/978-981-10-2955-4_17 (date of access: 17.01.2026).

[111] Mohammed M. S., Hamdey M. D., Kareem A. H., Majdi H. S. Investigation of copper backing plate effects in stainless steel welding distortion, heat distribution, and residual stress. *International Journal of Heat and Technology*. 2024. Vol. 42, no. 4. P. 1434–1446. URL: https://doi.org/10.18280/ijht.420433 (date of access: 17.01.2026).

these studies is on the welding of dissimilar metals or carbon steels[112],[113]. There are still only a limited number of studies specifically related to the welding of thin-walled elements made of austenitic stainless steel. This creates a need for further research into avoiding crater formation when welding thin-walled products with a rotation axis made of stainless steel. One of the most promising approaches to eliminating crater formation is to use a smooth increase and decrease in laser power at the beginning and end of the welding process, respectively. The use of zigzag power modulation allows to reduce the length of crystallization cracks in the crater and limit their penetration into the welded joint[114]. In addition, overlap welding and smoothing welds also help reduce the risk of craters and crystallization cracks forming[115]. Further research prospects include optimizing the profiles of increasing and decreasing the power of laser radiation during welding, taking into account the specific geometry of the joint and the properties of the material.

4. Development and testing of auxiliary technological equipment for laser welding

The efficiency of laser welding of thin-walled stainless steels is largely determined not only by the parameters of the welding modes, but also by the level of technological support for the process. Given the short lifetime of the weld pool (10-20 ms) and the limited length of the welded joint section, which requires gas protection no more than 30-40 mm long. Therefore, it is important to use gas protection devices that ensure stable conditions for the crystallization of the weld metal and prevent the formation of oxides and defects in welded joints.

An important auxiliary technological device is a clamping device designed for precise fixing and joining of welded edges. Its use will minimize gaps between welded parts, improve heat dissipation from the welding area, and reduce the probability of non-welds and thermal deformations.

To ensure process stability and high repeatability of girth welded joints, it is also necessary to use a precision rotator, which will ensure accurate positioning

[112] Kenda M., Klobčar D., Nagode A., Bračun D. Analysis and prevention of weld crater cracking in circumferential laser microwelding of automotive pressure sensors. *Engineering Failure Analysis*. 2021. Vol. 128. 105579. URL: https://doi.org/10.1016/j.engfailanal.2021.105579 (date of access: 17.01.2026).

[113] Gook S., Üstündag Ö., Gumenyuk A., Rethmeier M. Avoidance of end crater imperfections at high-power laser beam welding of closed circumferential welds. Welding in the World. 2019. Vol. 64, no. 2. P. 407–417. URL: https://doi.org/10.1007/s40194-019-00841-x (date of access: 17.01.2026).

[114] Kenda M., Klobčar D., Nagode A., Bračun D. Analysis and prevention of weld crater cracking in circumferential laser microwelding of automotive pressure sensors. *Engineering Failure Analysis*. 2021. Vol. 128. 105579. URL: https://doi.org/10.1016/j.engfailanal.2021.105579 (date of access: 17.01.2026).

[115] Gook S., Üstündag Ö., Gumenyuk A., Rethmeier M. Avoidance of end crater imperfections at high-power laser beam welding of closed circumferential welds. Welding in the World. 2019. Vol. 64, no. 2. P. 407–417. URL: https://doi.org/10.1007/s40194-019-00841-x (date of access: 17.01.2026).

of parts, uniform movement, and improve weld formation, especially at the beginning and end of the welded joint, where craters and other defects often occur.

The development of 3D models and working drawings of auxiliary technological equipment elements was carried out using the Autodesk Inventor CAD system.

4.1. Creation and testing of a gas protection device

To solve the problem of gas protection of the welding zone, a gas protection device for welded joints was designed (Fig. 14) and manufactured (Fig. 15). The design of the device allows the use of various protective gases, which are applied depending on the chemical composition of the materials being welded. The protective gas is supplied to the outer surface of the welded samples, to the molten metal bath spot, and to the welded seam. The gas protection device for laser processing consists of two parts.

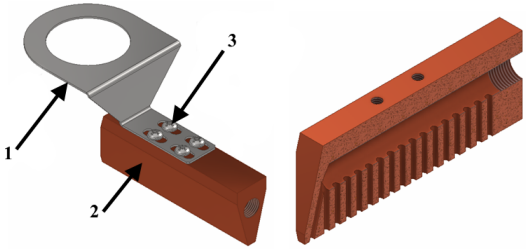

a **b**

Fig. 14. 3D model of a gas protection device for welded joints (a): 1 – protective gas distributor mounting, 2 – protective gas distributor, 3 – M4 screws; (b) cross-section of the protective gas distributor housing

Fig. 15. Manufactured gas protection device for welded joints

The gas protection distributor is a solid structure made of copper measuring 80×16×28 mm, has two side bevels at an angle of 75º for unhindered passage between the clamping plates of the clamping device, and a third bevel at an angle of 15º for docking with the nozzle of the laser processing head. The gas protection distributor body has a blind hole Ø8.6 mm and sixteen holes Ø2 mm perpendicular to it, as well as one hole Ø2 mm at an angle for supplying protective gas to the welding zone. The length of the holes is 13 mm, which ensures laminar flow of the protective gas and eliminates turbulence that can lead to air suction into the welding zone. The Ø8.6 mm hole has a G1/8 thread for connecting the fitting. There are also four M4 threaded holes for attaching the protective gas distributor holder. The distributor and gas protection holder are fastened to each other with four M4 screws. The protective gas distributor fastener is a bent thin-sheet part made of 0.8 mm thick corrosion-resistant steel. The part has 4 grooves for attaching to the gas protection distributor and one Ø33 mm hole for attaching to the laser processing head using a nozzle clamping nut. Figure 16 shows a schematic of the gas protection device attachment to the laser welding head.

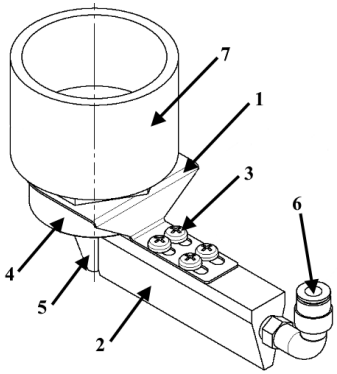

Fig. 16. Scheme of attaching the gas protection device to the laser welding head, where 1 – protective gas distributor attachment, 2 – protective gas distributor, 3 – M4 screws, 4 – nozzle clamping nut, 5 – nozzle, 6 – fitting, 7 – laser welding head housing

4.2. Creation and testing of a clamping device

In accordance with the requirements of EN ISO 15614-11:2015 on the manufacture of test welded joints, a preliminary design of laboratory equipment for the manufacture of flat and cylindrical samples from thin-sheet material using laser processing technologies was developed. Fig. 17 shows a 3D model of the developed technological equipment.

In accordance with the draft design, a clamping conductor was manufactured for welding test welded joints using mechanical processing such as milling, grinding, drilling, and welding.

The clamping device for welding flat and cylindrical samples consists of several parts and has dimensions of 650×170×675 mm (Fig. 18). Frame 1 is designed for mounting device elements on it. It is a welded structure made of a 25×25 square profile pipe. A base plate 7 and a screw mounting plate 8 for the drive of the movable clamp 4 are welded to two sides of the opposite edges. A profile pipe was chosen to reduce the weight of the frame structure. The base plates and screw mounting plate are machined and have parallel edges. The frame dimensions are 650×170×186 mm.

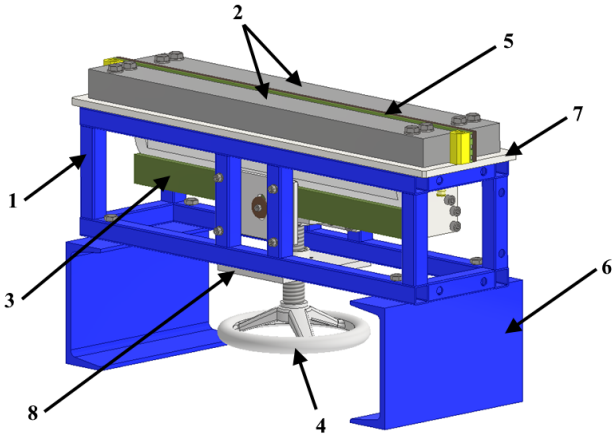

Fig. 17. 3D model of a clamping device for welding flat and cylindrical samples made of thin sheet material: 1 – frame; 2 – clamping plates; 3 – inner clamp (movable); 4 – movable clamp drive; 5 – weld joint orientation device; 6 – support elements; 7 – base plate; 8 – screw mounting plate

Frame 1 is installed on two support elements 6 made of channel bar No. 16, which are fixed on the assembly and welding table. To ensure uniform contact with the sample and prevent deformation during welding, clamping plates 2 made of 20 steel measuring 660×68×20 mm are used. Two fixed clamping plates with bevels towards the weld are installed on the base plate for unobstructed passage of the gas protection device.

The movable clamp 3 is a cylindrical element made of aluminum alloy D16T and is fixed with a screw on the underside of the clamping device. The diameter

of the body can vary depending on the diameter of the workpiece being welded. The clamp body has a gas protection system for the back of the weld, which consists of a protective gas supply channel and a weld cooling element. It provides reliable protection of liquid and hot (with a temperature above 500°C) metal from the surrounding atmosphere. A groove and a protective gas supply channel are provided for inserting the gas supply bar. The gas supply bar has 49 holes with a diameter of 2 mm for the passage of protective gas from the back side of the weld. The types of protective gas are selected depending on the chemical composition of the materials being welded. The shielding gas is supplied to the inner surface of the welded samples, the molten metal pool spot of the laser beam, and the welded seam (seam protection length up to 90 mm). The gas supply system is equipped with a 10 mm diameter hose connector (through which the gas is supplied). Gas consumption is 4–30 l/min at a pressure of 0.01–0.25 MPa. To reduce resistance when removing the welded cylindrical workpiece (part), flats are machined on both sides of the housing. The dimensions of the housing are 500 mm in length, 81 mm in diameter, and it weighs 6 kg.

Fig. 18. Clamping device for welding flat and cylindrical samples made of thin sheet material

The clamping device design also includes two cooling plates made of copper with a 4×2 mm groove for gas supply from the reverse side of the workpiece (part) with a length of 500 mm. The Ø1.5 mm holes for the protective gas outlet in the gas supply plate are made together with the holes in the cooling plates. The gas supply plate and the cooling plate are connected to each other in one part. Depending on the profile of the workpiece (part) being welded (flat or cylindrical), the plates are changed in the clamp body.

The welded joint alignment device is designed to set a guaranteed gap between the edges of the workpiece (part) before final compression and to align the edges along the axis of the clamping device in the manipulator coordinate system. The alignment device is set in the groove between the fixed clamping plates using pins mounted on the frame. Between the support plate and the clamping plate there is an alignment ruler – a steel strip 27×500 mm thick 0.15 – 0.35 mm, made of 65G steel. It is fixed by compression between the support and clamping plates. Figure 19 shows schemes of laser welding using a clamping device.

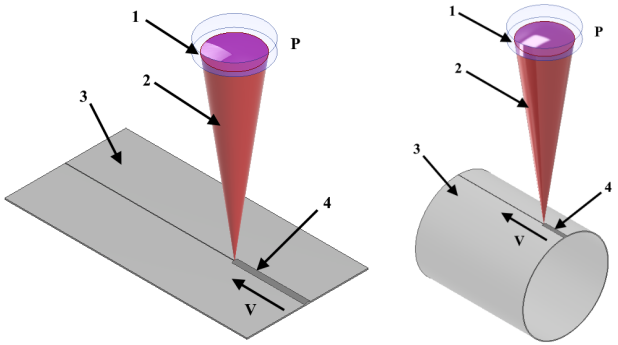

a b

Fig. 19. Schemes of laser welding using a clamping device: a) welding of flat parts, b) welding of cylindrical parts, where 1 – focusing lens, 2 – laser beam, 3 – workpiece to be welded, 4 – weld

To test the clamping device and gas protection device, experiments were conducted on welding 1.5 mm thick AISI 321 steel using various welding parameters. A DY044 Nd:YAG laser with a radiation power of up to 4.4 kW and a radiation wavelength of λ=1.06 μm, manufactured by Rofin-Sinar (Germany), was used for the research. The welding post is shown in Figure 20.

Test bead-on-plate welds were performed using different welding modes. Laser welding modes were optimized by visually inspecting the welded joint for defects in accordance with EN ISO 13919-1:2015 «Welding – Electron and laser-beam welded joints – Guidance on quality levels for imperfections – Part 1: Steel, nickel, titanium and their alloys». This standard provides for visual inspection for the presence of such defects in welded joints as: lack of fusion, lack of penetration, undercut, excessive convexity, excessive penetration, metal leakage, concavity of the root of the weld and its undercut, metal spatter. Based on the results of visual inspection, no defects were found, and three optimal

welding modes with the same linear energy were selected: 1) P = 1.5 kW, V = 1.5 m/min, 2) P = 2.5 kW, V = 2.5 m/min, 3) P = 3.5 kW, V = 3.5 m/min, welds No. 1, No. 7, and No. 8, respectively (Fig. 21).

a **b**

Fig. 20. Welding post with installed clamping device (a) and gas protection device (b)

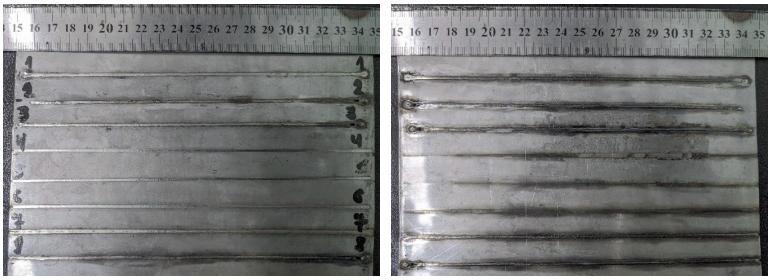

a **b**

Fig. 21. Welded AISI 321 steel bead-on-plate samples: (a) weld face, (b) root side

As can be seen from the images of welded samples, the clamping device for welding thin-sheet materials ensures constant uniform heat dissipation from the welding zone, uniform clamping of the welded sample along the entire length of the clamping conductor, as well as gas protection of the reverse side of welded joints. In turn, the gas protection device for the welding zone and the cooling metal of the weld also provides reliable gas protection, which allows to obtain welded joints without heat tint. Fig. 22 shows images from X-ray inspection, which show the absence of pores in the obtained welds.

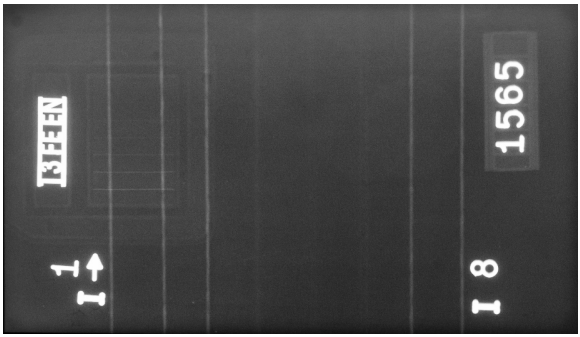

Fig. 22. X-ray image of the resulting bead-on-plate welds in 1.5 mm thick AISI 321 steel

4.3. Creation and testing of a precision rotator

For laser welding of girth welded joints of thin-walled products made of high-alloy steels, auxiliary precision technological equipment was developed and manufactured, which is a precision rotator (Fig. 23).

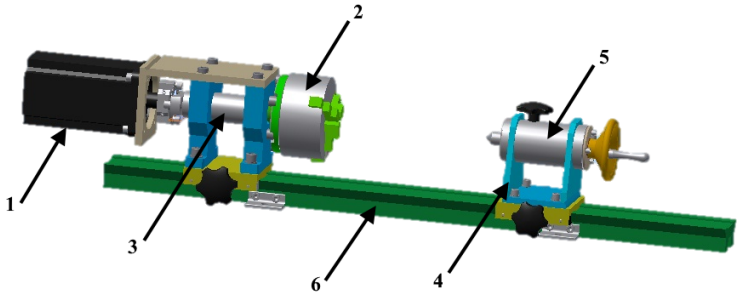

Fig. 23. 3D model of a precision rotator: 1 – servomotor; 2 – chuck for clamping rotating bodies; 3 – front headstock; 4 – rear headstock; 5 – rear headstock spindle for supporting rotating bodies; 6 – bed

Figure 24 shows the general view of the front headstock

The bracket is made of 10 mm thick steel plates welded at a 90° angle and machined in two mutually perpendicular planes for mounting the motor and fastening to the bearing housing. The bearing housing is mounted on a slide made of Steel 3 (mild steel). Its purpose is to allow the headstock to move along the machine bed. The bed profile resembles a dovetail. The bearing housing is made of 25 mm thick steel and accommodates bearings that support

the axis of rotation of the faceplate (Fig. 25, item 1). A Ø120 mm lathe chuck is mounted on the faceplate for clamping the workpieces. A coupling is installed on the faceplate shaft to connect it to the motor shaft. A spacer sleeve is installed between the housing elements and serves to protect the bearings from contamination (Fig. 25, item 2).

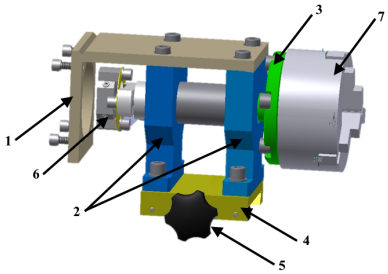

Fig. 24. General view of the front headstock: 1 – bracket; 2 – bearing housing; 3 – faceplate with shaft; 4 – slide; 5 – locking screw; 6 – coupling; 7 – chuck

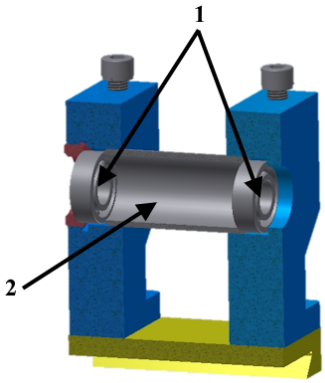

Fig. 25. Bearing housing, where 1 – bearings, 2 – spacer sleeve

Figure 26 shows a general sectional view of the rear headstock. The purpose of the rear headstock is to support the axis of the welded structure component. The clamping cone moves in the horizontal direction by means of a sleeve actuated by a screw–nut pair during rotation of the handwheel.

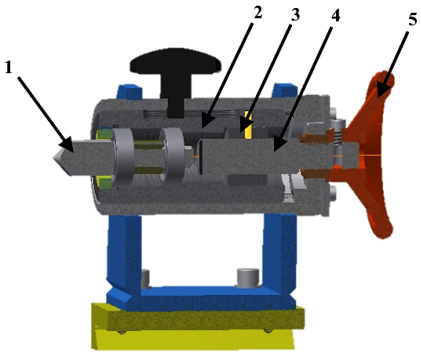

Fig. 26. Sectional view of the rear headstock: 1 – clamping cone; 2 – sleeve; 3, 4 – screw–nut pair; 5 – handwheel.

Figure 27 shows the completed precision rotator.

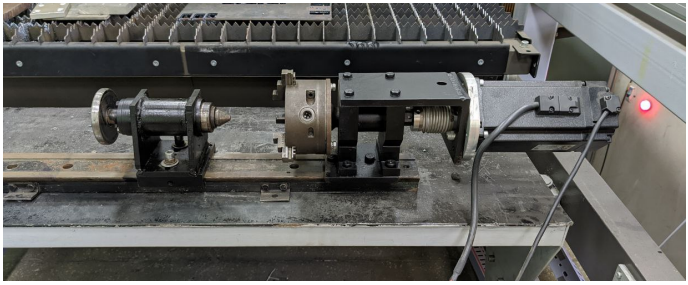

Fig. 27. Precision rotator

Due to the presence of a frame, the precision rotator allows welding parts up to 450 mm long. The chuck for clamping rotating bodies can accommodate parts with a diameter of 6 to 90 mm. The servomotor is synchronized with the laser welding system, ensuring positioning accuracy of 1 mm and repeatability of no worse than ±0.08 mm.

The precision rotator allows laser welding according to the scheme shown in Figure 28.

As a test of the precision rotator, laser welding of a bellows with a flange made of stainless steel AISI 304 was performed (Fig. 29).

Laser welding was performed in pulse mode with a pulse frequency of 1000 Hz. The welding head has a focal length of 200 mm (ΔF = +5 mm). The maximum power of laser radiation is P = 240 W. The welding speed

V = 0.5 m/min (1 rev/5 sec). To protect the welding area, a protective gas – high-purity argon – was used. The gas consumption was 20 l/min.

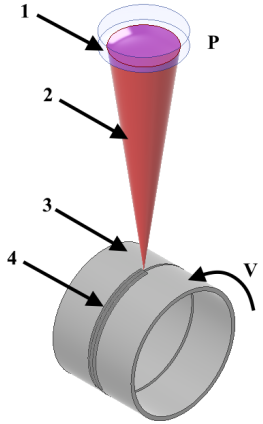

Fig. 28. Laser welding scheme on the precision rotator, where 1 – focusing lens, 2 – laser beam, 3 – workpiece to be welded, 4 – weld

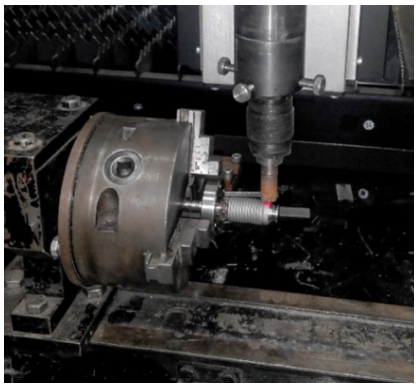

Fig. 29. Welding bellows on a precision rotator

To prevent metal spatter and crater formation, a smooth start and smooth stop at the end of the welded joint welding process was used, as well as a smooth increase and decrease in laser radiation power at the beginning and end of the welding process. The parameters of the laser welding parameters are given in Table 2.

Table 2

Laser welding parameters for bellows

Stages of welding	Welding speed, V m/min	Welding power, $P_{average}$ W	Movement relative to the axis of the part, degrees
Power increase	0,5	20	3
	0,5	40	3
	0,5	60	3
Main seam	0,5	120	365
Power decrease	0,5	60	3
	0,5	40	3
	0,5	20	3

As a result of laser welding using a precision rotator, a welded joint of the bellows with the flange was obtained (Fig. 30).

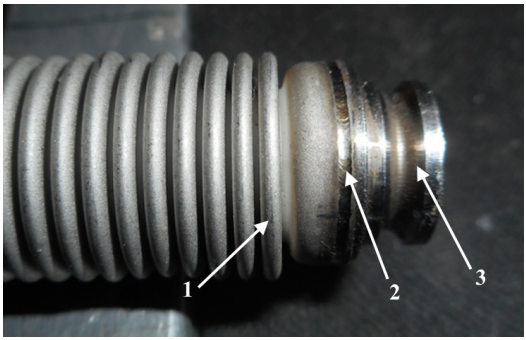

Fig. 30. Result of laser welding of a bellows made of AISI 304 steel with a wall thickness of 0.25 mm with a flange made of AISI 304 steel, where 1 – bellows, 2 – weld, 3 – flange

The rotator allows to make girth welded joints, ensuring uniform weld penetration. An additional advantage is the presence of a servo motor, which provides precise control of the rotation speed and allows to automate the welding process, increasing its stability and productivity. This, in turn, makes it possible to develop laser welding technology for other products used in various industries, such as aircraft manufacturing, mechanical engineering, etc.

CONCLUSIONS

Analysis of scientific works on laser welding of thin-walled products has made it possible to identify a number of pressing issues and to develop and

manufacture the necessary auxiliary technological equipment to overcome them:

1) The clamping device allows the production of flat and cylindrical samples from thin-sheet material that meet the requirements of EN ISO 15614-11:2015, from steels and alloys across a wide range of technological parameters. This is achieved thanks to the clamping device's design, which includes an internal clamping device with a shielding gas system for the weld root, a copper cooling plate, and an alignment ruler for the edges of the workpieces to be welded.

2) The gas shielding device provides reliable protection of the welding zone and the cooling weld metal due to its shape, which allows it to be used between closely spaced clamping plates of the clamping device. Additionally, the diameter and length of the gas supply holes have a ratio greater than 1:5, which ensures a laminar flow of the shielding gas and prevents the formation of turbulence.

3) The precision rotator enables the formation of girth welds with diameters up to 90 mm, ensuring uniform weld penetration thanks to the servomotor, which provides precise control of the rotational speed and allows automation of the welding process, thereby enhancing its stability and productivity. Another advantage is the ability to synchronize the servomotor with the laser control unit, which makes it possible to apply a technological technique such as smooth increase and decrease laser radiation power at the beginning and end of the welding process to prevent crater formation in the welds.

The results of testing the developed auxiliary technological equipment confirmed its effectiveness. The use of this equipment will allow solving a wide range of tasks relevant for the rocket, chemical, medical, defense and other industries that use thin sheet metal in production.

SUMMARY

The effectiveness of laser welding of thin-walled corrosion-resistant steels is determined not only by the welding parameters but also by the level of technological support of the process. This study analyzes the main challenges in laser welding of thin-walled components, including insufficient shielding of the weld zone, difficulty in achieving precise edge alignment, thermal deformations, and defect formation at the beginning and end of the weld. Based on this analysis, the key steps to eliminate these issues and improve process stability were identified. A set of auxiliary technological equipment was developed and manufactured, including a clamping device, a shielding gas device, and a precision rotator. The proposed clamping device ensures accurate positioning of components, minimization of gaps, and effective heat dissipation. The shielding gas device creates a stable

laminar flow of protective gas over the weld and the cooling metal. The precision rotator provides uniform formation of girth welds and enables automation of the welding process. The developed equipment was experimentally tested under real laser welding conditions. The results demonstrated that the obtained welds comply with the requirements of EN ISO 15614-11:2015, confirming the effectiveness of the proposed technical solutions.

Bibliography

1. Altenbach H., Eremeyev V. Thin-walled structural elements: Classification, classical and advanced theories, new applications. shell-like structures / ed. by H. Altenbach, V. Eremeyev. Cham: Springer International Publishing, 2017. URL:https://doi.org/10.1007/978-3-319-42277-0_1 (date of access: 17.01.2026)

2. Shelyagin V.D., Khaskin V.Yu., Bernatsky A.V., Siora, A.V.. Laser welding of thin-wall filter elements of steel 08Kh18N10T. *The Paton Welding Journal,* 2017. Vol. 4. P. 49-52. URL: https://doi.org/10.15407/tpwj2017.04.10 (date of access: 17.01.2026).

3. Kuczek T. Application of manufacturing constraints to structural optimization of thin-walled structures. Engineering Optimization. 2015. Vol. 48, no. 2. P. 351–360. URL: https://doi.org/10.1080/0305215x.2015.1017350 (date of access: 17.01.2026).

4. McNair S. a. M., Chaharsooghi A. S., Carnevale M., Rhead A., Onnela A., Daguin J., Cichy K., et al. Manufacturing technologies and joining methods of metallic thin-walled pipes for use in high pressure cooling systems. *The International Journal of Advanced Manufacturing Technology*. 2021. Vol. 118, no. 3–4. P. 667–681. URL: https://doi.org/10.1007/s00170-021-07982-8 (date of access: 17.01.2026).

5. Wang K., Li L. Structural analysis and optimal design of a spherical thin-walled stainless steel water tank without reinforced tie ribs. *Journal of Vibroengineering*. 2024. Vol. 20, no. 4. P. 983-1000. URL: https://doi.org/10.21595/jve.2024.23812 (date of access: 17.01.2026).

6. Michler T. Austenitic stainless steels. *Reference Module in Materials Science and Materials Engineering.* 2016. Vol. 1, no. 6. URL: https://doi.org/10.1016/b978-0-12-803581-8.02509-1 (date of access: 17.01.2026).

7. Ibrahim O., Ibrahim I., Khalifa T. Impact behavior of different stainless steel weldments at low temperatures. *Engineering Failure Analysis.* 2010. Vol. 17, no. 5. P. 1069–1076. URL: https://doi.org/10.1016/j.engfailanal.2009.12.006 (date of access: 17.01.2026).

8. Lv X., Chen S., Wang Q., Jiang H., Rong L. Temperature dependence of fracture behavior and mechanical properties of AISI 316 austenitic stainless

steel. *Metals*. 2022. Vol. 12, no. 9. 1421. https://doi.org/10.3390/met12091421 (date of access: 17.01.2026).

9. ASTM A480/A480M-22a. Standard specification for general requirements for flat-rolled stainless and heat-resisting steel plate, sheet, and strip. Effective from 2023-06-02. Official edition. URL: https://store.astm.org/a0480_a0480m-22a.html (date of access: 17.01.2026).

10. Kumar K., Kumar C. S., Masanta M., Pradhan S. A review on TIG welding technology variants and its effect on weld geometry. *Materials Today Proceedings*. 2021. Vol. 50. P. 999–1004. URL: https://doi.org/10.1016/j.matpr.2021.07.308 (date of access: 17.01.2026).

11. Advancing implantable medical device reliability with enhanced laser joining technology. *Home – Medical Design Briefs*. URL: https://www.medicaldesignbriefs.com/component/content/article/52177-advancing-implantable-medical-device-reliability-with-enhanced-laser-joining-technology (date of access: 17.01.2026).

12. Sabdin S. D., Hussein N. I. S., Sued M. K., Ayof M. N. Joining of thin plates using various arc welding heat sources–A Review. *Journal of Advanced Manufacturing Technology (JAMT)*. 2018. Vol. 12, no. 1. P. 357-370. URL: https://jamt.utem.edu.my/jamt/article/view/4005 (date of access: 17.01.2026).

13. Khoshnaw F. Welding of metallic materials methods, metallurgy, and performance. Elsevier, 2023. 608 p.URL: https://doi.org/10.1016/c2020-0-03713-8 (date of access: 17.01.2026).

14. Manh N. H., Van Anh N., Van Tuan N., Xu B., Akihisa M. Research and development of a novel TIG welding torch for joining thin sheets. *Applied Sciences.* 2019. Vol. 9, no, 23. 5260. URL: https://doi.org/10.3390/app9235260 (date of access: 17.01.2026).

15. Yurchenko, Yu. V., et al. Analysis of actual problems of laser welding of stainless steel thin sheets and search for solutions. *International Journal of Science Engineering and Technology*. 2024. Vol. 12, no. 5. P. 1–9. URL: https://doi.org/10.61463/ijset.vol.12.issue5.289 (date of access: 17.01.2026).

16. Bala Y., Rajendran D. K. Global welding market growth. *Automation in Welding Industry: Incorporating Artificial Intelligence, Machine Learning and Other Technologies*. 2024. P. 229–243. URL: https://doi.org/10.1002/9781394172948.ch13 (date of access: 17.01.2026).

17. Buang A. S., Bakar M. S. A., Rohani M. Z. A review of trend advanced welding process and welding technology in industries. *International Journal of Technical Vocational and Engineering Technology.* 2024. Vol. 5, no. 1. P. 133-145. URL: https://journal.pktm.com.my/index.php/ijtvet/article/download/103/72 (date of access: 17.01.2026).

18. Rahadian N. Advancements in welding technology: A comprehensive review of techniques, materials, and applications. *Journal PEP Bandung.* 2025. Vol. 2, no. 1. P. 62-110. https://ejournal.pepbandung.ac.id/index.php/gm/article/view/12 (date of access: 17.01.2026).

19. EN ISO 6520-1:2007. Welding and allied processes – Classification of geometric imperfections in metallic materials – Part 1: Fusion welding. Effective from 2014-02-15 URL: https://uscc.ua/uploads/page/images/normativnye%20dokumenty/dstu/vigotovlennya-mk-mizhnarodna-gilka-standarty/78-dstu-iso-5817-2016-zvaryuvannya.pdf (date of access: 17.01.2026).

20. Kenda M., Klobčar D., Nagode A., Bračun D. Analysis and prevention of weld crater cracking in circumferential laser microwelding of automotive pressure sensors. *Engineering Failure Analysis*. 2021. Vol. 128. 105579. URL: https://doi.org/10.1016/j.engfailanal.2021.105579 (date of access: 17.01.2026).

21. Jian G. A. O., Xiaojiao S. O. N. G., Lihua P. A. N., Ling X. I. A., Jie X. U. Study on the quality control of arc crater in laser welding girth weld. *Electric Welding Machine.* 2022. Vol. 52, *no.*5. P. 112-116. URL: http://doi.org/10.7512/j.issn.1001-2303.2022.05.16 (date of access: 17.01.2026).

22. Lai W. J., Ganguly S., Suder W. Study of the effect of inter-pass temperature on weld overlap start-stop defects and mitigation by application of laser defocusing. *The International Journal of Advanced Manufacturing Technology*. 2021. Vol. 114. P. 117–130. URL: https://doi.org/10.1007/s00170-021-06851-8 (date of access: 17.01.2026).

23. Zhang P., Jia Z., Yu Z., Shi H., Li S., Wu D., Tian Y. A review on the effect of laser pulse shaping on the microstructure and hot cracking behavior in the welding of alloys. *Optics & Laser Technology.* 2021. Vol. 140. 107094. URL: https://doi.org/10.1016/j.optlastec.2021.107094 (date of access: 17.01.2026).

24. Ramon J., Basu R., Voort G. V., Bolar G. A comprehensive study on solidification (hot) cracking in austenitic stainless steel welds from a microstructural approach. *International Journal of Pressure Vessels and Piping*. 2021. Vol. 194. 104560. https://doi.org/10.1016/j.ijpvp.2021.104560 (date of access: 17.01.2026).

25. Gook S., Üstündag Ö., Gumenyuk A., Rethmeier M. Avoidance of end crater imperfections at high-power laser beam welding of closed circumferential welds. Welding in the World. 2019. Vol. 64, no. 2. P. 407–417. URL: https://doi.org/10.1007/s40194-019-00841-x (date of access: 17.01.2026).

26. Mahajanam S., Heidersbach K. Corrosion studies of heat-tinted austenitic stainless steel. *Materials Performance*. 2021. Vol. 60, no. 5. P. 42–47. URL:https://doi.org/10.5006/mp2021_60_5-42 (date of access: 17.01.2026).

27. Kearns J. R. The corrosion of heat tinted austenitic stainless alloys. *Corrosion*. 1985. P. 1–11. URL: https://doi.org/10.5006/c1985-85050 (date of access: 17.01.2026).

28. Zhang Z., Jing H., Xu L., Han Y., Zhao L., Zhou C. Effects of nitrogen in shielding gas on microstructure evolution and localized corrosion behavior of duplex stainless steel welding joint. *Applied Surface Science*. 2017. Vol. 404. P. 110–128. URL: https://doi.org/10.1016/j.apsusc.2017.01.252 (date of access: 17.01.2026).

29. Hinds G., Wickström L., Turnbull A. Influence of weld preparation procedure and heat tinting on sulfide stress corrosion cracking of duplex stainless steel. *Corrosion*. 2015. P. 1–15. URL: https://doi.org/10.5006/c2015-06084 (date of access: 17.01.2026).

30. Schricker K., Baumann A., Bergmann J. P. Local shielding gas supply in remote laser beam welding. *Journal of Manufacturing and Materials Processing*. 2021. Vol. 5, no. 4. 139. URL: https://doi.org/10.3390/jmmp5040139 (date of access: 17.01.2026).

31. Chen K., Hu Z. H., Huang R., Li M. X., Xiao R. S. Outflow Forms of Shielding Gas in Laser Welding by Schlieren. *Journal of Beijing University of Technology.* 2007. Vol. 33, no. 12. P. 1340-1344. URL: https://journal.bjut.edu.cn/bjgydxxb/en/article/pdf/preview/10.3969/j.issn.0254-0037.2007.12.020.pdf (date of access: 17.01.2026).

32. Zou J., Xie S., Kong H., Liu T., Fang C., Wu Q. Active control effect of shielding gas flow on high-power fiber laser welding plume. *Journal of Laser Applications*. 2024. Vol. 36, no. 3. 032011. URL: https://doi.org/10.2351/7.0001407 (date of access: 17.01.2026).

33. Tani G., Ascari A., Campana G., Fortunato A. A study on shielding gas contamination in laser welding of non-ferrous alloys. *Applied Surface Science*. 2007. Vol. 254, no. 4. P. 904–907. URL: https://doi.org/10.1016/j.apsusc.2007.08.067 (date of access: 17.01.2026).

34. Wang S., Zhou Y., Alam M. M., Yang H. Turbulent intensity and Reynolds number effects on an airfoil at low Reynolds numbers. *Physics of Fluids*. 2014. Vol. 26, no. 11. 115107. URL: https://doi.org/10.1063/1.4901969 (date of access: 17.01.2026).

35. Blackburn J., Allen C., Hilton P., Li L. Nd:YAG laser welding of titanium alloys using a directed gas jet. *Journal of Laser Applications*. 2010. Vol. 22, no. 2. P. 71–78. URL: https://doi.org/10.2351/1.3455825 (date of access: 17.01.2026).

36. Vyskoč M., Sahul M., Dománková M., Jurči P., Sahul M., Vyskočová M., Martinkovič M. The effect of process parameters on the microstructure and mechanical properties of AW5083 aluminum laser weld joints. *Metals*. 2020.

Vol. 10, no. 11. 1443. URL: https://doi.org/10.3390/met10111443 (date of access: 17.01.2026).

37. Hamadou M., Fabbro R., Caillibotte G., Chouf K., Briand F. Study of assist gas flow behavior during laser welding. *ICALEO 2002: 21st International Congress on Laser Materials Processing and Laser Microfabrication*. October 14–17, 2002 Scottsdale, Arizona, USA. URL: https://doi.org/10.2351/1.5066140 (date of access: 17.01.2026).

38. Campana G., Ascari A., Fortunato A., Tani G. Hybrid laser-MIG welding of aluminum alloys: The influence of shielding gases. *Applied Surface Science*. 2008. Vol. 255, no. 10. P. 5588–5590. URL: https://doi.org/10.1016/j.apsusc.2008.07.169 (date of access: 17.01.2026).

39. Grevey D., Sallamand P., Cicala E., Ignat S. Gas protection optimization during Nd:YAG laser welding. *Optics & Laser Technology*. 2004. Vol. 37, no.8. P. 647–651. URL: https://doi.org/10.1016/j.optlastec.2004.08.015 (date of access: 17.01.2026).

40. Elshawesh F., Elhoud A. Role of heat tint on pitting corrosion of 304 austenitic stainless steel in chloride environment (No. INIS-FR--3844). Societe de Chimie Industrielle (SCI), 28 Rue Saint Dominique, F-75007 Paris (France). 2004. URL: https://inis.iaea.org/records/016t7-4rr25 (date of access: 17.01.2026).

41. Tran N., Nguyen V., Nguyen V., Trung T., DO, Nguyen V., Nguyen V. Effects of heat input and backing gas on bead geometry and weld heat tint in sanitary tube welding. *Thermo.* 2025. Vol. 5, no. 4. 49. URL: https://doi.org/10.3390/thermo5040049 (date of access: 17.01.2026).

42. Ciofu F., Nioata A., Luca L. Duplex stainless steel corrosion resistance. *Fascicle of Management of Technological Engineering*. 2010. Vol. 9. URL: https://imt.uoradea.ro/auo.fmte/files-2010-v2/TCM/Ciofu%20Florin%20L2.pdf (date of access: 17.01.2026).

43. Olsson C., Landolt D. Passive films on stainless steels–chemistry, structure and growth. *Electrochimica Acta*. 2003. Vol. 48, no. 9. P. 1093–1104. URL: https://doi.org/10.1016/s0013-4686(02)00841-1 (date of access: 17.01.2026).

44. Morcillo M., Díaz I., Cano H., Chico B., De La Fuente D. Atmospheric corrosion of weathering steels. Overview for engineers. Part I: Basic concepts. *Construction and Building Materials*. 2019. Vol. 213. P. 723–737. URL: https://doi.org/10.1016/j.conbuildmat.2019.03.334 (date of access: 17.01.2026).

45. Aljohani T. A., Alateyah A., El-Sanabary S., El-Garaihy W. Corrosion of weldments. *Welding of Metallic Materials: Methods, Metallurgy, and Performance*. 2023. P. 565–588. URL: https://doi.org/10.1016/b978-0-323-90552-7.00010-9 (date of access: 17.01.2026).

46. Zhu L., Cui Z., Cui H., Wang X., Li Y. The effect of applied stress on the crevice corrosion of 304 stainless steel in 3.5 wt% NaCl solution. *Corrosion Science*. 2022. Vol. *196*. 110039. URL: https://doi.org/10.1016/j.corsci.2021.110039 (date of access: 17.01.2026).

47. Wang X., Sun Y., He P., Tan X., Zhou Q., Wu W., Lv C., Li J., Jiang Y. Understanding the pitting behavior of laser welds in different austenitic stainless steels: From the perspective of pitting initiation. *Corrosion Science*. 2023. Vol. 224, 111483. URL: https://doi.org/10.1016/j.corsci.2023.111483 (date of access: 17.01.2026).

48. Sun L., Chen S., Qiu J., Zhao T. Research on the mechanism and detection method of intergranular corrosion of AISI 304 stainless steel by electrochemical techniques in heat exchanger equipment. *Journal of Materials Engineering and Performance*. 2022. Vol. 32, no. 2. P. 534–543. URL: https://doi.org/10.1007/s11665-022-07132-5 (date of access: 17.01.2026).

49. Kappes M. A. Localized corrosion and stress corrosion cracking of stainless steels in halides other than chlorides solutions: a review. *Corrosion Reviews*. 2019. Vol. 38, no. 1. P. 1–24. URL: https://doi.org/10.1515/corrrev-2019-0061 (date of access: 17.01.2026).

50. Aghuy A. A., Zakeri M., Moayed M., Mazinani M. Effect of grain size on pitting corrosion of 304L austenitic stainless steel. *Corrosion Science*. 2015. Vol. 94. P. 368–376. URL: https://doi.org/10.1016/j.corsci.2015.02.024 (date of access: 17.01.2026).

51. Srinivasan N. Sensitization of Austenitic Stainless steels: current developments, trends, and future directions. *Metallography Microstructure and Analysis*. (2021). Vol. 10, no. 2. P. 133–147. URL: https://doi.org/10.1007/s13632-021-00724-y (date of access: 17.01.2026).

52. Shit G., Mariappan K., Ningshen S. Improvement of sensitization and intergranular corrosion of AISI type 304L stainless steel through thermo-mechanical treatment. *Corrosion Science*. 2023. Vol. 213. 110975. URL: https://doi.org/10.1016/j.corsci.2023.110975 (date of access: 17.01.2026).

53. Vakili M., Koutník P., Kohout J., Gholami Z. Analysis, assessment, and mitigation of stress corrosion cracking in austenitic stainless steels in the oil and gas sector: a review. *Surfaces*. 2024. Vol. 7, no. 3. P. 589–642. URL: https://doi.org/10.3390/surfaces7030040 (date of access: 17.01.2026).

54. Derakhshan E. D., Yazdian N., Craft B., Smith S., Kovacevic R. Numerical simulation and experimental validation of residual stress and welding distortion induced by laser-based welding processes of thin structural steel plates in butt joint configuration. *Optics & Laser Technology*. 2018. Vol. 104. P. 170–182. URL: https://doi.org/10.1016/j.optlastec.2018.02.026 (date of access: 17.01.2026).

55. Vykhtar B., Lingner M., Richter A. M., Hoops F. Monitoring and local gas shielding at laser-based welding of titanium alloys. *Procedia CIRP*. 2022. Vol. 111. P. 532–535. URL: https://doi.org/10.1016/j.procir.2022.08.085 (date of access: 17.01.2026).

56. Huang H., Tsutsumi S., Wang J., Li L., Murakawa H. High performance computation of residual stress and distortion in laser welded 301L stainless sheets. *Finite Elements in Analysis and Design*. 2017. Vol. 135. P. 1–10. URL: https://doi.org/10.1016/j.finel.2017.07.004 (date of access: 17.01.2026).

57. Murakawa H. Residual stress and distortion in laser welding. *Handbook of Laser Welding Technologies*. 2013. P. 374–400. URL: https://doi.org/10.1533/9780857098771.2.374 (date of access: 17.01.2026).

58. Liu Z., Jin X., Li J., Hao Z., Zhang J. Numerical simulation and experimental analysis on the deformation and residual stress in trailing ultrasonic vibration assisted laser welding. *Advances in Engineering Software*. 2022. Vol. 172. 103200. URL: https://doi.org/10.1016/j.advengsoft.2022.103200 (date of access: 17.01.2026).

59. Tayebi M., Soltani H. M., Rajaee A. Laser welding. In *IntechOpen eBooks*. 2022. URL: https://doi.org/10.5772/intechopen.102456 (date of access: 17.01.2026).

60. Kumar B., Bag S., Mahadevan S., Paul C., Das C., Bindra K. On the interaction of microstructural morphology with residual stress in fiber laser welding of austenitic stainless steel. *CIRP Journal of Manufacturing Science and Technology*. 2021. Vol. 33. P. 158–175. URL: https://doi.org/10.1016/j.cirpj.2021.03.009 (date of access: 17.01.2026).

61. Chiocca A., Frendo F., Bertini L. Residual stresses influence on the fatigue strength of structural components. *Procedia Structural Integrity*. 2022. Vol. 38. P. 447–456. URL: https://doi.org/10.1016/j.prostr.2022.03.045 (date of access: 17.01.2026).

62. Hummelshøj T. S., Christiansen T. L., Somers M. A. Lattice expansion of carbon-stabilized expanded austenite. *Scripta Materialia*. 2010. Vol. 63, no. 7. P. 761–763. URL: https://doi.org/10.1016/j.scriptamat.2010.05.031 (date of access: 17.01.2026).

63. Lin Y., Chou C. A new technique for reducing the residual stress induced by welding in type 304 stainless steel. *Journal of Materials Processing Technology*. 1995. Vol. 48, no. 1–4. P. 693–698. URL: https://doi.org/10.1016/0924-0136(94)01710-i (date of access: 17.01.2026).

64. Mandal N.R. Welding Residual Stress and Distortion. *Ship Construction and Welding. Springer Series on Naval Architecture, Marine Engineering, Shipbuilding and Shipping.* 2017. Vol. 2. Springer URL: https://doi.org/10.1007/978-981-10-2955-4_17 (date of access: 17.01.2026).

65. Mohammed M. S., Hamdey M. D., Kareem A. H., Majdi H. S. Investigation of copper backing plate effects in stainless steel welding distortion, heat distribution, and residual stress. *International Journal of Heat and Technology*. 2024. Vol. 42, no. 4. P. 1434–1446. URL: https://doi.org/10.18280/ijht.420433 (date of access: 17.01.2026).

Information about the author:
Yurchenko Yurii Viktorovych,
Postgraduate Student,
Lead Engineer at the Department
of the Specialized High-Voltage Engineering and Laser Welding,
E. O. Paton Electric Welding Institute
of the National Academy of Sciences of Ukraine,
11, Kazymyra Malevycha str., Kyiv, 03680, Ukraine